Received: 3 December 2019 | Revised: 25 May 2020 | Accepted: 28 May 2020

DOI: 10.1111/bph.15158

RESEARCH PAPER

Artesunate interacts with the vitamin D receptor to reverse sepsis-induced immunosuppression in a mouse model via enhancing autophagy

Shenglan Shang[1,2] | Jiaqi Wu[1] | Xiaoli Li[1] | Xin Liu[1] | Pan Li[1,3] | Chunli Zheng[4] | Yonghua Wang[4] | Songqing Liu[2] | Jiang Zheng[1] | Hong Zhou[1,3,5]

[1]Medical Research Center, Southwest Hospital, Third Military Medical University (Army Medical University), Chongqing, China

[2]Department of Pharmacy, Southwest Hospital, Third Military Medical University (Army Medical University), Chongqing, China

[3]Chongqing municipal Enterprise Technology Center, Chongqing Shenghuaxi Pharmaceutical Co., Ltd., Chongqing, China

[4]Key Laboratory of Basic Pharmacology of Ministry of Education and Joint International Research Laboratory of Ethnomedicine of Ministry of Education, Zunyi Medical University, Zunyi, Guizhou, China

[5]Key Laboratory of Resource Biology and Biotechnology in Western China, Ministry of Education, School of Life Sciences, Northwest University, Xi'an, Shanxi, China

Correspondence
Hong Zhou, Southwest Hospital, Third Military Medical University (Army Medical University), Chongqing 400038, China; Chongqing Shenghuaxi Pharmaceutical Co., Ltd., No.8 Jiangqiao Road, Nan'an District, Chongqing 401336, China; Key Laboratory of Basic Pharmacology of Ministry of Education and Joint International Research Laboratory of Ethnomedicine of Ministry of Education, Zunyi Medical University, Zunyi, Guizhou 563003, China.
Email: zhouh64@163.com

Jiang Zheng, Medical Research Center, Southwest Hospital, Third Military Medical University (Army Medical University), Chongqing 400038, China.
Email: zhengj99219@163.com

Songqing Liu, Department of Pharmacy, Southwest Hospital, Third Military Medical University (Army Medical University),

Background and Purpose: Immunosuppression is the predominant cause of mortality for sepsis because of failure to eradicate pathogens. No effective and specific drugs capable of reversing immunosuppression are clinically available. Evidences implicate the involvement of the vitamin D receptor (NR1I1) in sepsis-induced immunosuppression. The anti-malarial artesunate was investigated to determine action on sepsis-induced immunosuppression.

Experimental Approach: The effect of artesunate on sepsis-induced immunosuppression was investigated in mice and human and mice cell lines. Bioinformatics predicted vitamin D receptor as a candidate target for artesunate, which was then identified using PCR and immunoblotting. *Vdr*, *Atg16l1* and *NF-κB p65* were modified to investigate artesunate 's effect on pro-inflammatory cytokines release, bacterial clearance and autophagy activities in sepsis-induced immunosuppression.

Key Results: Artesunate significantly reduced the mortality of caecal ligation and puncture (CLP)-induced sepsis immunosuppression mice challenged with *Pseudomonas aeruginosa* and enhanced pro-inflammatory cytokine release and bacterial clearance to reverse sepsis-induced immunosuppression *in vivo* and *in vitro*. Mechanistically, artesunate interacted with vitamin D receptor, inhibiting its nuclear translocation, which influenced *ATG16L1* transcription and subsequent autophagy activity. Artesunate inhibited the physical interaction between vitamin D receptor and *NF-κB p65* in LPS-tolerant macrophages and then promoted the nuclear translocation of *NF-κB p65*, which activated the transcription of *NF-κB p65* target genes such as pro-inflammatory cytokines.

Conclusion and Implications: Our findings provide evidence that artesunate interacted with vitamin D receptor to reverse sepsis-induced immunosuppression in an autophagy and NF-κB-dependent manner, highlighting a novel approach for sepsis treatment and drug repurposing of artesunate has a bidirectional immunomodulator.

Abbreviations: anti-PD-1, anti-programmed cell death receptor-1; AS, artesunate; ATG16L1, autophagy related 16 like 1; Baf, bafilomycin A1; ChIP, chromatin immunoprecipitation; CLP mice, caecal ligation and puncture (CLP)-induced sepsis immunosuppression mice; CLP, caecal ligation and puncture; co-IP, coimmunoprecipitation; LC3B, protein 1 light chain 3; PA, *Pseudomonas aeruginosa*; PMs, peritoneal macrophages; RAW264.7, macrophage-like RAW cells; RXR, retinoid X receptor; TCMSP, traditional Chinese medicine systems pharmacology database and analysis platform; TEM, transmission electron microscopy; TLR4, toll-like receptor 4; VDR, vitamin D receptor; V_{D3}, 1α,25$(OH)_2D_3$ (calcitriol); 3-MA, 3-methyladenine.

Chongqing 400038, China.
Email: songqingliu@hotmail.com

Funding information
Special Basic Science and Cutting-edge Research Project of Chongqing, Grant/Award Number: cstc2015jcyjBX0049; the fourth batch of "Thousand People Innovation and Entrepreneurship Talents Fund" in Guizhou Province, Shijingshan's Tutor Studio of Pharmacology, Grant/Award Number: GZS-2016(07); Major National Science and Technology Program of China for Innovative Drug, Grant/Award Number: 2017ZX09101002-002-009; National Natural Science Foundation of China, Grant/Award Numbers: 81872914, 81772137, 81673495

1 | INTRODUCTION

Sepsis is a leading cause of death worldwide (Angus & van der Poll, 2013); it arises when hosts response to pathogen infections such as bacterial, fungal, viral and parasitic infection and then injury their own tissues and organs (Hotchkiss, Monneret, & Payen, 2013b). At present, Coronavirus Disease 2019 (COVID-19) caused by severe acute respiratory syndrome coronavirus 2 (SARS-CoV-2), a newly recognized virus, has spread rapidly around the world and has infected closed to more than 6,600,000 people and killed more than 380,000 until June 4, 2020, because of no specific and effective drug.

The course of sepsis involves the innate and acquired immune systems, in which mononuclear phagocytes play a crucial role. Although the timeline of immunological alterations in sepsis is not well understood, increasing evidences suggest that sepsis development involves two distinct stages, an initial cytokine storm (hyper-inflammation) and subsequent immunosuppression (hypo-inflammation), which exist concomitantly and dominate in different stages (Hotchkiss, Monneret, & Payen, 2013a; Hutchins, Unsinger, Hotchkiss, & Ayala, 2014). The uncontrolled cytokine storm is responsible for deaths that occur within the first few days, whereas immunosuppression predominantly causes mortality during the later stages. In fact, more than 70% of patients die after the first 3 days of sepsis, possibly because of increased susceptibility to weakly virulent pathogens or opportunistic bacteria (e.g. *Pseudomonas aeruginosa* [PA]), indicating the host's failure to eradicate invading pathogens (Hotchkiss et al., 2013a; Skrupky, Kerby, & Hotchkiss, 2011). For patients in the immunosuppression stage, less than 5% of monocytes/macrophages produce cytokines, indicative of the disordered immune response in sepsis (Hotchkiss et al., 2013a; Hutchins et al., 2014). This impaired function of monocytes/macrophages is closely associated with the decreased removal of bacteria. Drugs based on the inhibiting critical pro-inflammatory mediators have failed; therefore, current sepsis research is focusing on therapeutic strategies to improve immunosuppression (Cohen, 2002; Hotchkiss et al., 2013a; Kox, Volk, Kox, & Volk, 2000; Prucha, Zazula, & Russwurm, 2017).

Autophagy is a fundamental cellular process involved in the defence against intracellular pathogen infection (Casanova, 2017). Although contradictory findings have been reported (Ho et al., 2016), accumulating evidence suggests that autophagy plays a key role in sepsis and might be a target for sepsis-induced immunosuppression (Ren, Zhang, Wu, & Yao, 2017). Thus, focusing on the autophagy axis might reveal the mechanism of sepsis-induced immunosuppression and lead to novel immunoregulatory therapy for sepsis.

Artesunate (AS) is an effective and reliable anti-malarial drug with low toxicity (Burrows, Chibale, & Wells, 2011; Clark et al., 2004) that possesses anti-inflammation and other effects (Efferth, Dunstan, Sauerbrey, Miyachi, & Chitambar, 2001; Li et al., 2008; Miranda et al., 2013; Wang et al., 2017). Previously, we showed that artesunate protects septic

What is already known

- Immunosuppression is the predominant cause of mortality during the later phase of sepsis.
- Vitamin D receptor (VDR; NR1I1) activation is closely related to the pathophysiological duration of sepsis.

What does this study add

- Artesunate reverses sepsis-induced immunosuppression resulting from caecal ligation and puncture in mice.
- Artesunate interacts with VDR to reverse sepsis-induced immunosuppression in an autophagy and NF-κB-dependent manner.

What is the clinical significance

- Autophagy inhibited by VDR receptor overexpression might be a drug target for reversing sepsis-induced immunosuppression.
- Artesunate is a bidirectional immunomodulator to treat sepsis caused by pathogens and deserves further investigation.

animals by inhibiting pro-inflammatory cytokine release in the cytokine storm stage (Li et al., 2008), suggesting an anti-inflammatory effect during the cytokine storm phase. In the present study, a caecal ligation and puncture (CLP)-induced sepsis immunosuppression mouse model was used to investigate the effect of artesunate on sepsis-induced immunosuppression. An **LPS**/endotoxin-tolerant cell model was established to reveal the underlying mechanism.

2 | METHODS

2.1 | Animals

All animal care and experimental procedures were approved by Laboratory Animal Welfare and Ethics Committee of the Third Military Medical University (AMUWEC2020015). Animal studies are reported in compliance with the ARRIVE guidelines (Kilkenny et al., 2010) and with the recommendations made by the *British Journal of Pharmacology*. BALB/c mice (RRID:IMSR_ORNL:BALB/cRl; sex: half male and half female; weight: 18–22 g; age: 6–8 weeks) were obtained from Beijing HFK Bioscience (Beijing, China) and housed in a pathogen-free facility with a 12-h artificial light–dark cycle in the Third Military Medical University. All the mice were provided with food and purified water ad libitum. There were no more than five mice in each cage.

2.2 | Cell lines, culture and isolation of peritoneal macrophages from mice

The murine macrophage-like cell line RAW264.7 (CLS Cat#400319/p462_RAW-2647, RRID:CVCL_0493) cells and human monocyte THP-1 (CLS Cat# 300356/p804_THP-1, RRID:CVCL_0006) cells were purchased from the American Type Culture Collection (Manassas, VA, USA). RAW264.7 cells were cultured in DMEM supplemented with 10% low-LPS FBS (Hyclone, Logan, UT, USA) and 1% penicillin/streptomycin (regular medium) at 37°C in a humidified 5% CO_2 atmosphere. THP-1 cells were cultured in RPMI 1640 (Hyclone) regular medium in suspension. THP-1 derived macrophages were obtained by differentiating THP-1 cells with phorbol 12-myristate 13-acetate (PMA) (Sigma-Aldrich, St. Louis, MO, USA) treatment at 100 nM for 24 h according to the previous study (Li et al., 2017).

Mouse peritoneal macrophages (PMs) were obtained from BALB/c mice. Each mouse was injected intraperitoneally with 3 ml of 3% thioglycolate (Sigma-Aldrich) on day 1 and killed using isoflurane on day 3. After intraperitoneal injection of 5 ml of DMEM regular medium, the peritoneal cells were collected into cell culture dishes. Two hours later, the floating cells were removed by washing the cells with PBS. The attached cells were considered to be peritoneal macrophages (purity was about 90%) and were subjected to further experiments. The primary mouse macrophages or cell lines were maintained in regular medium at 37°C in a humidified 5% CO_2 atmosphere. All the reagents and utensils used in the experiment were LPS-free.

2.3 | Bacterial strain and preparation of bacterial suspension

The clinical isolate of *Pseudomonas aeruginosa* was kindly provided by Prof. Peiyuan Xia (Southwestern Hospital, Chongqing, China). A single colony was picked from viable, growing cells on a Mueller-Hinton (MH) agar plate, transferred to 5 ml of liquid MH medium and cultivated aerobically at 37°C in an orbital shaking incubator for 4 h. The cultures were transferred to 100 ml of fresh MH medium for another 12 h. At an OD600 of 0.6–0.8, when the bacterial culture was within the logarithmic phase of growth, as measured using a SmartSpec 3000 spectrophotometer (Bio-Rad, Hercules, CA, USA), the suspension was centrifuged at 1,500×*g* for 10 min to harvest the pellet. After washing twice, the pellet was resuspended in sterile normal saline. The bacteria were diluted in sterile normal saline to achieve the final concentration (colony-forming unit [CFU]·ml^{-1}), which was calculated according to the bacterial growth curve determined in our laboratory (Concentration = (9.7544 × OD − 1.4965) × 10^8 CFU·ml^{-1}).

2.4 | Establishment of caecal ligation and puncture (CLP)-induced sepsis immunosuppression mouse model and artesunate treatment

Currently, CLP in rodents is regarded as a gold standard in sepsis research (Rittirsch, Huber-Lang, Flierl, & Ward, 2009). CLP immunosuppression mice (CLP mice) with a second bacterial infection model were established in our laboratory and were described previously (Deng et al., 2017). Briefly, CLP mice were established by ligating the distal 1.0 cm of the caecum and puncturing once with a No. 16 steel needle and then intravenously injecting *Pseudomonas aeruginosa* (with 2.5 × 10^9 CFU·kg^{-1}) at 24 h after CLP surgery (Figure 1a).

Artesunate (injection preparation, Guilin Pharma Corp, Guangxi, People's Republic of China National Medicine Standard H10930195) was added into the attached injection containing 5% sodium bicarbonate, shaken for 2 min until completely dissolved and then diluted in sterile normal saline to achieve the final concentration. Artesunate (10 mg·kg^{-1}) was intramuscularly injected at 22, 26, 48 and 72 h following CLP surgery. The survival rate of the mice was observed for 7 days. CLP mice were killed at 4 h after *Pseudomonas aeruginosa* injection. The blood, lungs and spleen tissues were collected for CFU count assays and ELISA.

2.5 | Establishment of LPS-tolerance cell model

LPS tolerance is used extensively to simulate the sepsis-induced immunosuppression phase in vitro (Li et al., 2013). Herein, a cell model of LPS tolerance was established in mouse peritoneal macrophages and RAW264.7 cells and human THP-1 cells. Briefly, cells were cultured with LPS (0111: B4, 5 ng·ml^{-1}, Sigma-Aldrich) for 4 h. Then the culture supernatant was replaced followed by the addition of LPS (100 ng·ml^{-1}) to establish the LPS-tolerant cell model.

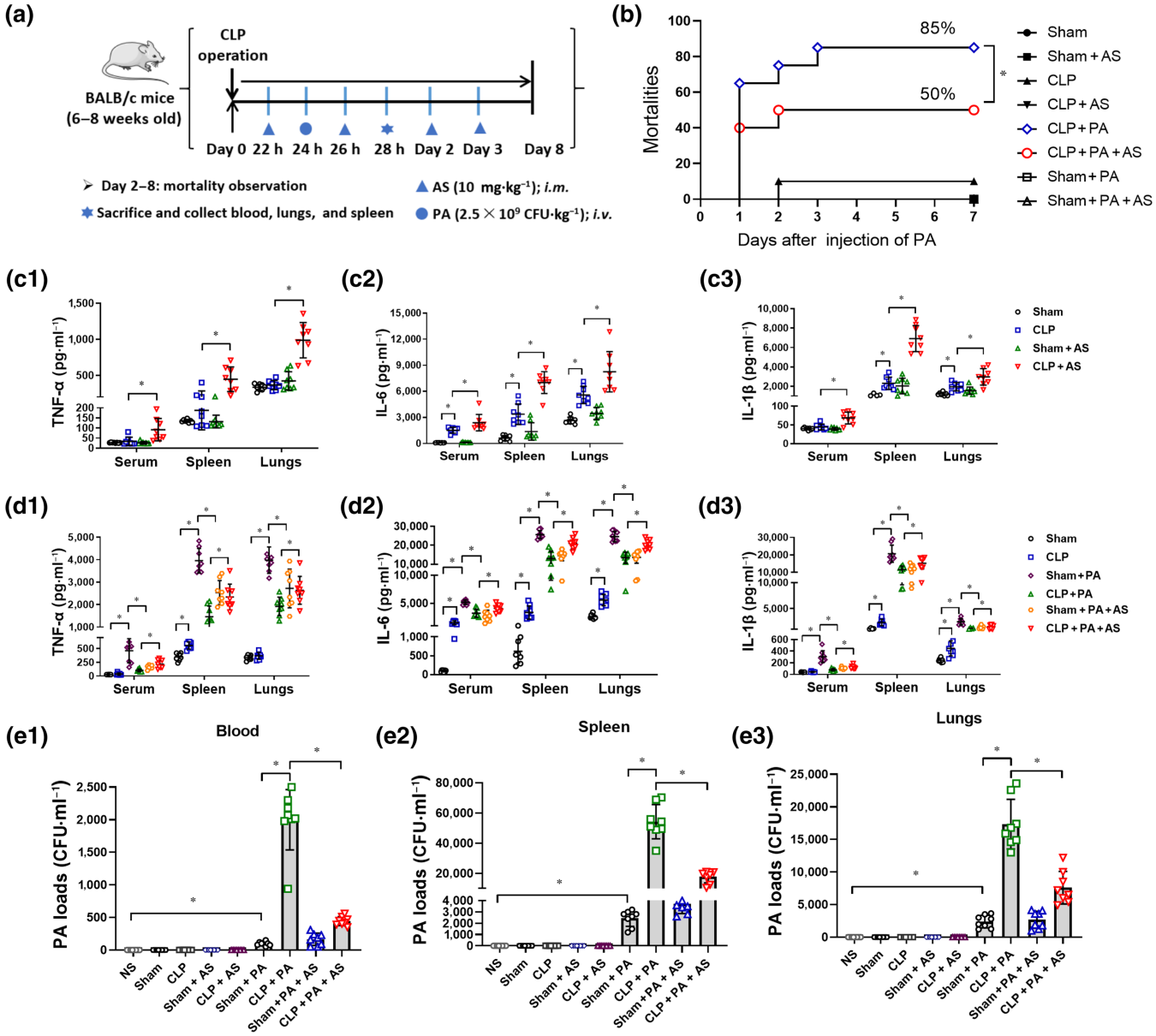

FIGURE 1 Artesunate (AS) reverses sepsis-induced immunosuppression in caecal ligation and puncture (CLP) mice. (a) Schematic diagram of the establishment of the CLP mouse model with secondary bacterial infection. (b) Mortality of CLP mice challenged with *Pseudomonas aeruginosa* (PA) and treated by AS (10 mg·kg^{-1}) (n = 20). (c) Effect of AS treatment on the level of TNF-α (c1), IL-6 (c2) and IL-1β (c3) in the serum, spleen and lungs of CLP mice (n = 8). (d) Effect of AS treatment on the level of TNF-α (d1), IL-6 (d2), and IL-1β (d3) in the serum, spleen and lungs of CLP mice challenged with PA (n = 8). (e) Effect of AS treatment on the bacterial load in the blood (e1), spleen (e2) and lungs (e3) at 4 h after the CLP mice were challenged with PA (n = 8). Kaplan–Meyer log-rank test (b); one-way ANOVA followed by Tukey's post hoc test (c–e); $^{*}P < 0.05$

2.6 | Artesunate, autophagy inhibitors and 1α,25 $(OH)_2D_3$ treatment *in vitro*

For artesunate treatment, artesunate (5, 10 and 20 μg·ml^{-1}) was added with LPS (5 ng·ml^{-1}) and LPS (100 ng·ml^{-1}) simultaneously. For autophagy inhibitors treatment, 3-methyladenine (3-MA, 5 mM, Sigma-Aldrich), bafilomycin A1 (Baf, 10 ng·ml^{-1}, MedChemExpress, Monmouth Junction, NJ, USA), and LY294002 (10 μM, Sigma-Aldrich) were added 2 h before the first LPS (5 ng·ml^{-1}) and also simultaneously with artesunate treatment. The treatment of 1α,25$(OH)_2D_3$ (V_{D3}) (100 nM, Solarbio, Beijing, China) was the same as the autophagy inhibitors. The supernatants and cells were collected at 6 h after the last LPS (100 ng·ml^{-1}) addition.

2.7 | siRNA, lentivirus and their transfections *in vitro*

Control siRNA-A (Santa Cruz Biotechnology, Dallas, TX, USA), *Vdr* siRNA (Santa Cruz Biotechnology) and *Atg16l1* esiRNA (endoribonuclease-prepared siRNA; Sigma-Aldrich) were used. RAW264.7 cells were transfected with 50 nM of target siRNA or control siRNA using Lipofectamine 3000 (Thermo Fisher Scientific, Waltham, MA,

USA) and Opti-MEM I reduced serum medium (Thermo Fisher Scientific) for 6 h. After recovering overnight, the cells were subjected to further treatment.

The DNA fragments encoding mouse *Vdr* (NM_009504) or *NF-κB p65* (NM_009045) were synthesized and inserted into the lentivirus vector (#GV358, GeneChem) by GeneChem Corporation (Shanghai, China). The resulting recombinant lentivirus was named *Vdr*-OE or *p65*-OE. The negative control (#CON238, GeneChem) was named NC-OE. The shRNA targeting mouse *Vdr* (5′-CCTCAAACTCTGATCTGTA-3′), *NF-κB p65* (5′-CCCTCAGCACCATCAACTTTG-3′) and the negative control shRNA (5′-TTCTCCGAACGTGTCACGT-3′) were designed, synthesized and inserted into the lentivirus vector (#GV248, GeneChem) by GeneChem Corporation. The resulting recombinant lentiviruses were named *Vdr*-KD, *p65*-KD and NC-KD.

For lentivirus transfection, RAW264.7 cells were cultured to 50% confluence and transfected with the lentivirus according to the protocol in the Lentivirus Operation Manual for 6 h. After 3 days of renewed culture in regular DMEM, the cells were subjected to further treatment.

2.8 | shRNA transfection *in vivo*

The lentiviruses *Vdr*-KD and NC-KD were diluted to a total volume of 200 μl containing 4×10^7 TU. BALB/c mice were transfected through tail intravenous injection as reported previously (Morizono et al., 2005). One week later, the mice were killed and spleen tissues were collected to detect the infection efficiency. Further CLP modelling and artesunate treatment were employed in the transfected mice and their tissues were collected for cytokines and western blotting assays.

2.9 | Interacting molecular prediction for artesunate

Interacting molecular prediction for artesunate was performed against 5,311 proteins using the weighted ensemble similarity algorithm (Zheng et al., 2015) assembled in the traditional Chinese medicine systems pharmacology database and analysis platform (TCMSP) (Ru et al., 2014). Weighted ensemble similarity was developed to determine a drug's affiliation for a target by evaluation of the overall similarity (ensemble) rather than a single ligand judgement, which allowed us to discover scaffold hopping ligands. The ligand structural and physicochemical features of artesunate were calculated using Chemical Development Kit (CDK) (Steinbeck et al., 2003) and Dragon software and then used to evaluate the ensemble similarity between artesunate and the ligands of candidate targets. Finally, the standardized ensemble similarities of Chemical Development Kit and Dragon were integrated using a Bayesian network to rank the predicted targets.

2.10 | Transmission electron microscopy

RAW264.7 cells were treated as indicated above and fixed in 2.5% glutaraldehyde at 4°C overnight and then post fixed with 2% osmium tetroxide for 1.5 h at room temperature. After fixation, the cells were embedded in resin, sectioned and stained with uranyl acetate/lead citrate. The sections were examined under a transmission electron microscope (JEM-1400PLUS, Japan) at 60 kV.

2.11 | Immunofluorescence assay

The immuno-related procedures used comply with the recommendations made by the *British Journal of Pharmacology* (Alexander et al., 2018). RAW264.7 cells or peritoneal macrophages plated on the coverslips for 2 h and treated as indicated in Section 2.5. The coverslips were fixed in 4% paraformaldehyde for 20 min and permeabilized in 0.5% Triton X-100 (Solarbio) which dissolved in PBS for 5 min (20 min for nucleoprotein staining). Then the coverslips were blocked for 1 h at 37°C in PBS containing 3% BSA and 0.1% Triton X-100 and incubated with primary antibodies (Table S1) at 4°C overnight, followed by incubation with secondary antibodies. The cells on coverslips were counterstained with 2-(4-amidinophenyl)-1*H*-indole-6-carboxamidine (DAPI) (Beyotime, Shanghai, China). Confocal images were captured using a Zeiss LSM780 confocal microscope (Jena, Germany) with a Plan-Apo Chromat 63×/1.40 oil objective.

2.12 | MTT assay

RAW264.7 cells (5×10^4 cells per well) were plated in 96-well plates in regular medium. After overnight culture, the cells were washed with PBS and incubated with a series concentration of LPS or other treatments for 4 or 24 h. Subsequently, 20 μl of the methyl thiazolyl tetrazolium (MTT) solution (5 mg·ml^{-1}) was added to the medium in a total volume of 200 μl. The cells were incubated for 4 h at 37°C in a humidified 5% CO_2 atmosphere. The supernatant was removed and 150 μl of DMSO was added to each well to dissolve the produced formazan crystals. The extinction was measured at 490 nm using a SmartSpec 3000 spectrophotometer (Bio-Rad).

2.13 | Bacterial load assay

For the mouse tissue samples, at the indicated time points after *Pseudomonas aeruginosa* injection, the blood, lungs and spleen were collected. Blood or homogenates of cells, lungs and spleen tissues were serially diluted. Subsequently, 100 μl of the diluents was added to nutrient agar plates and cultured for 18 h. Images of the agar plates and CFU counts were obtained using a G6 automated colony counter (Shineso Science & Technology, Hangzhou, China).

For cell samples, 2 h after challenged with *Pseudomonas aeruginosa*, the cells were collected and washed with PBS three times. The cells were disrupted by 2 min of ultrasonication (ultrasonic time 5 s/gap time 10 s cycling, power 100 W) in an ice bath and then centrifuged under 4°C at 800×*g* for 5 min. The precipitate was resuspended in MH medium and serially diluted.

2.14 | Binding assay

Microlon ELISA Plates were coated with antibody against vitamin D receptor (VDR) (anti-VDR antibody) (Cell Signaling Technology Cat# 12550, RRID:AB_2637002) overnight at 4°C, followed by three washes with PBS. The cell lysate containing the total proteins, including the VDR protein, was added to the plates. After incubating at 37°C for 2 h, the VDR protein was captured by the anti-VDR antibody coated on the plates. Subsequently, the plates were washed three times and V_{D3} (Selleck, Houston, TX, USA) was added. After incubating at 37°C for 2 h, the plates were washed three times, and fluorophore-conjugated artesunate (designed and synthesized by Chongqing Canbipharma Technology, Chongqing, China) was added. After incubating at 37°C for 2 h, the plates were washed three times and the fluorescence intensity was observed using a Spectra Max i3x Multifunctional enzyme marker (Molecular Devices, San Jose, CA, USA) with an excitation wavelength of 360 nm and an emission wavelength of 455 nm. Artesunate conjugated with fluorophore 12-(7-oxycoumarinyl-ethoxy) dihydroartemisinin was named artesunate I and artesunate conjugated with 12-(-1*H*-benzo [de] isoquinoline-1, 3(2*H*)-dione-2-ethoxy) dihydroartemisinin was named artesunate II.

2.15 | Cytokines and NF-κB p65 assays

The supernatants were collected from cell cultures. Serum was separated from collected blood samples. For mouse tissue samples, 1 g of lungs and spleen tissue was homogenized and centrifuged and the supernatants were collected. The levels of cytokines such as TNF-α, IL-6 and IL-1β in all samples were determined using the appropriate ELISA kits (Thermo Fisher Scientific), according to the manufacturers' protocols. For NF-κB p65 levels in the nucleus and nucleoproteins were extracted and detected using a Trans-AM NF-κB kit (Active Motif, Carlsbad, CA, USA).

2.16 | Quantitative real-time PCR

Total RNAs were extracted from cells and tissues using the MagMAX total RNA isolation Kit (Thermo Fisher Scientific) and transcribed into cDNAs using Prime Script (Takara, Dalian, China). Using respective primers (Table S2), quantitative real-time PCR (qPCR) was performed using a 7900HT Fast Real-Time PCR system or ABI 7500 Real-Time PCR system (Applied Biosystems, Darmstadt, Germany). Expression levels were normalized to the expression of β-actin mRNA. Reactions were performed in duplicate using Tli RNaseH plus and universal PCR master mix (Takara). The relative expression was calculated by the $2^{(-\Delta\Delta Ct)}$ method (Livak & Schmittgen, 2001).

2.17 | Western blotting

Cell proteins and mice spleens were extracted using RIPA (Beyotime). Nuclear and cytoplasmic proteins were isolated using nucleoprotein extraction kits (Keygen Biotech, Beijing, China). The proteins were then quantified using a bicinchoninic acid (BCA) kit (Beyotime). Thirty micrograms of each protein sample were separated by 12% SDS-PAGE and transferred to a polyvinylidene difluoride membrane. The membranes were blocked with 5% BSA and incubated with primary antibodies (Table S1) overnight at 4°C. The membranes were rinsed five times with PBS containing 0.1% Tween 20 and incubated for 1 h with the appropriate HRP-conjugated secondary antibody at 37°C. Membranes were extensively washed with PBS containing 0.1% Tween 20 three times. Chemiluminescence-marked images were developed using the Enhanced Chemiluminescent Substrate (PerkinElmer, Norwalk, CT, USA) with a ChemiDoc™ Touch Imaging System (Bio-Rad) and analysed using the Image Lab package (Bio-Rad).

2.18 | ChIP assays

RAW264.7 cells were washed with cold PBS and crosslinked with 1% formaldehyde. The reaction was stopped using 0.125 M of glycine. The cells were then sonicated in chromatin immunoprecipitation (ChIP) lysis buffer to generate 600 bp of fragments, followed by overnight incubation with anti-VDR antibodies (Abcam, Cambridge, UK) at 4°C. The obtained DNA was subjected to semiquantitative or quantitative PCR analysis. Specific primers (Table S3) were used to amplify the VDR-binding region from the promoter of the *ATG16L1* gene, according to a previously described method (Wu et al., 2015). The ChIP assay was performed using the Pierce Agarose ChIP kit and following the manufacturer's instructions (Thermo Pierce, Rockford, IL, USA) (Bretin et al., 2016).

2.19 | Coimmunoprecipitation assay

Nuclear and cytoplasmic proteins from RAW264.7 cells were isolated using nucleoprotein extraction kits (Keygen Biotech, Jiangsu, China). Protein (1 mg) was incubated with anti-VDR antibodies (Cell Signaling Technology) at 4°C overnight. Immune complexes were collected using the Protein A/G beads and subjected to SDS-PAGE and western blotting as described in Section 2.17. Coimmunoprecipitation (co-IP) was performed according to the manual of the Protein A/G Magnetic Beads kit (Thermo Fisher Scientific).

2.20 | Statistical analysis

The data and statistical analysis comply with the recommendations of the *British Journal of Pharmacology* on experimental design and analysis in pharmacology (Curtis et al., 2018), with the exception that the analysis was not blinded. Each experiment involved at least five independent samples (equal size) per randomized group and that statistical analysis was done using these independent values. The statistical analysis was undertaken only for studies where each group size was at least $n = 5$.

Sample sizes were based upon our prior experience using the same paradigms (Deng et al., 2017; Kuang et al., 2018; Li et al., 2010). No outliers were excluded in the data analysis and presentation. The control and test values in PCR were normalized to an internal standard (such as *Actb* and *GAPDH*) to reduce variance. For binding assay and immunofluorescence assay, all values (control and test) were normalized to the mean value of the experimental control group to set the *Y*-axis, so the control group value was 1. The units for these normalized data in the *Y*-axis were the fold of the control group's mean value. The units for the other data were the exact unit of the assay but not fold control. The statistical analyses were performed using GraphPad Prism 8.0.2 (263) (RRID:SCR_002798; GraphPad Software, Inc., La Jolla, CA, USA). The Kaplan–Meyer log-rank test was used for the survival analysis of the mouse model of sepsis. All data were expressed as the mean ± SD. A Student's *t* test was used when comparing two values (two tailed, two-sample equal variance). The comparisons among multiple groups were performed with a one-way ANOVA. If appropriate (only if *F* in ANOVA achieved the "chosen" necessary level of statistical significance and there was no significant variance inhomogeneity), this was followed by Tukey's post hoc test. For each parameter of the data presented, * indicates $P < 0.05$.

2.21 | Nomenclature of targets and ligands

Key protein targets and ligands in this article are hyperlinked to corresponding entries in http://www.guidetopharmacology.org, the common portal for data from the IUPHAR/BPS Guide to PHARMACOLOGY (Harding et al., 2018) and are permanently archived in the Concise Guide to PHARMACOLOGY 2019/20 (Alexander et al., 2019).

3 | RESULTS

3.1 | Artesunate reverses sepsis-induced immunosuppression in caecal ligation and puncture (CLP) mice

Treatment with artesunate decreased the mortality of CLP mice challenged with *Pseudomonas aeruginosa* from 85% to 50% (Figure 1b), suggesting that artesunate could protect against CLP-induced immunosuppression in mice. In CLP mice without *Pseudomonas aeruginosa* challenge, the levels of **TNF-α**, **IL-1β** and **IL-6** were extremely low in the serum, spleen and lungs. However, their levels increased significantly in artesunate-treated CLP mice (Figure 1c). Furthermore, the cytokine levels in CLP mice challenged with *Pseudomonas aeruginosa* were also much lower compared with those in sham mice challenged with *Pseudomonas aeruginosa*, demonstrating that bacterial challenge did not induce pro-inflammatory cytokine release in sepsis-induced immunosuppressed mice. Noteworthily, artesunate treatment significantly augmented the cytokine levels in CLP mice challenged with *Pseudomonas aeruginosa* (Figure 1d). The bacterial loads increased markedly in the tissues of CLP mice challenged with *Pseudomonas aeruginosa* compared with those in the sham mice, demonstrating that the CLP mice had a lower bacterial clearance ability. However, artesunate significantly decreased the bacterial load in CLP mice challenged with *Pseudomonas aeruginosa* (Figure 1e). The aforementioned results suggested that artesunate could protect against sepsis-induced immunosuppression by increasing pro-inflammatory cytokine release and decreasing the bacterial load.

3.2 | Artesunate increases pro-inflammatory cytokines release and bacterial clearance in LPS-tolerant macrophages

Based on the concentration–effect relationship between LPS and cytokine production (Figure 2a), incubation in 5 $ng \cdot ml^{-1}$ of LPS for 4 h followed by 100 $ng \cdot ml^{-1}$ of LPS was determined to induce an LPS-tolerant phenotype (tolerant cells) (Figure 2b). Compared with cells treated with only 100 $ng \cdot ml^{-1}$ of LPS (LPS cells), tolerant cells pretreated with 5 $ng \cdot ml^{-1}$ of LPS followed by 100 $ng \cdot ml^{-1}$ of LPS released much less TNF-α and IL-6 (Figure 2c). However, artesunate dose-dependently increased TNF-α and IL-6 release in tolerant cells (Figure 2d). The results showed that the bacterial loads in LPS-tolerant cells increased relative to LPS cells at 2 h after *Pseudomonas aeruginosa* challenge. Significantly, artesunate decreased the bacteria load in tolerant cells (Figure 2e). Subsequently, the human monocyte cell line THP-1 and THP-1 derived macrophages were employed to confirm that artesunate had a similar effect on human macrophages. Identical results for the mRNA levels of *TNF-α* and *IL-6* and bacterial clearance were obtained in THP-1 cells and THP-1 derived macrophages, too (Figure 2f,g). The concentrations of LPS (2.5–200 $ng \cdot ml^{-1}$) and artesunate (0.625–40 $\mu g \cdot ml^{-1}$) used in the experiment did not affect cell viability, therefore the above effect was not related to LPS or artesunate toxicity (Figure S1) (Li et al., 2008). These results were consistent with the findings *in vivo*, demonstrating that artesunate reversed sepsis-induced immunosuppression by enhancing pro-inflammatory cytokines release and bacterial clearance by macrophages.

3.3 | Vitamin D receptor (VDR) is predicted to be an interaction candidate of artesunate

To further investigate the molecular mechanism of artesunate, the possibly interacting candidates were predicted. First, the top 20 candidates (Figure 3a) were screened using RT-PCR and western blotting. Among them, the most significant and stable change was observed in the mRNA and protein levels of VDR, which remarkably increased in tolerant cells and were decreased by artesunate treatment (Figure 3b,c).

Second, *Vdr* expression in RAW264.7 was modified. A *Vdr* siRNA and a lentiviral vector harbouring an RNAi sequence against *Vdr* were transfected into RAW264.7 cells to knock down *Vdr* expression (*Vdr*-KD cells) (Figure S2a). Knockdown of *Vdr* abrogated the LPS-tolerant phenotype,and artesunate addition had no effect (Figure 3d). A lentiviral vector harbouring the *Vdr* gene was transfected into RAW264.7 cells to overexpress *Vdr* (*Vdr*-OE cells) (Figure S2b). The results showed that the

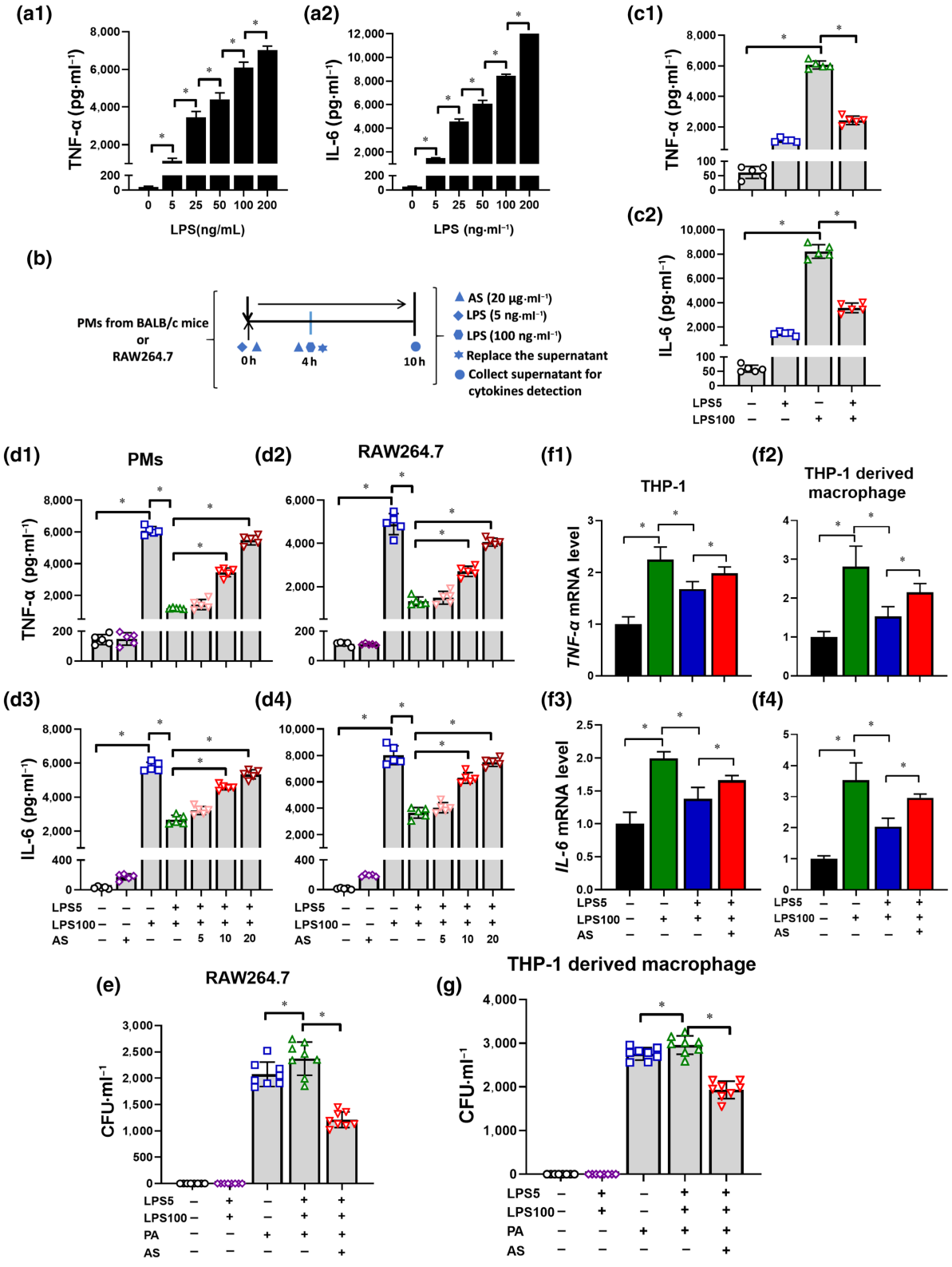

FIGURE 2 Artesunate (AS) increases pro-inflammatory cytokines release and bacterial clearance within LPS-tolerant macrophages (n = 4). (a) LPS increased the release of TNF-α (a1) and IL-6 (a2) from peritoneal macrophages (PMs) in a dose-dependent manner. (b) Schematic diagram of the establishment of the LPS-tolerant macrophage model. (c) The level of TNF-α (c1) and IL-6 (c2) in LPS-tolerant PMs (n = 5). (d) Effect of AS (5, 10 and 20 μg·ml^{-1}) treatment on the level of TNF-α (d1, d2) and IL-6 (d3, d4) in LPS-tolerant PMs and RAW264.7 cells (n = 5). (e) Effect of AS treatment (20 μg·ml^{-1}) on the bacterial load in LPS-tolerant RAW264.7 cells (n = 8). (f) Effect of AS (20 μg·ml^{-1}) treatment on the mRNA level of *TNF-α* (f1, f2) and *IL-6* (f3, f4) in LPS-tolerant THP-1 monocytes and THP-1 derived macrophages (n = 5). (g) Effect of AS treatment (20 μg·ml^{-1}) on the bacterial load in LPS-tolerant THP-1 derived macrophages (n = 8). One-way ANOVA followed by Tukey's post hoc test; $^{*}P < 0.05$

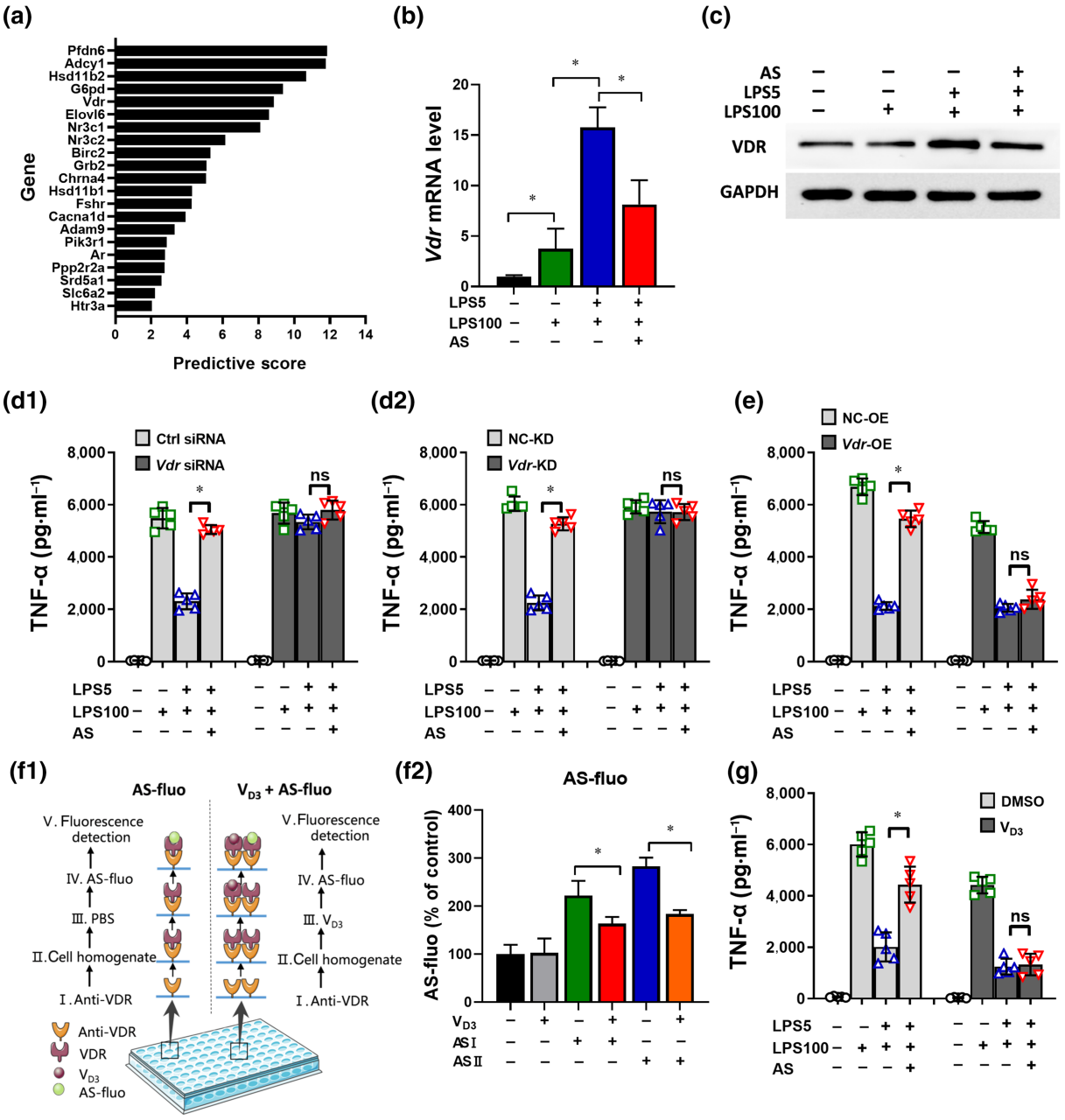

FIGURE 3 The vitamin D receptor is predicted to be an interactor candidate of artesunate (AS). (a) A total of 20 underlying signal molecules were selected via the traditional Chinese medicine systems pharmacology database and analysis platform (TCMSP). (b) Effect of AS on the relative mRNA levels of *Vdr* (n = 5). (c) Effect of AS on the protein levels of VDR (n = 5). (d) Effect of *Vdr* siRNA (d1) and *Vdr*-KD lentiviral vector (d2) on TNF-α levels in LPS-tolerant RAW264.7 cells treated with AS (n = 5). (e) Effect of *Vdr*-OE lentiviral vector on TNF-α level in LPS-tolerant RAW264.7 cells treated with AS (n = 5). (f1) Schematic diagram of the binding assay designed in our laboratory. (f2) Effect of V_{D3} on the binding of AS and VDR tracked by AS fluorophores (n = 5). AS with fluorophore 12-(7-oxycoumarinyl-ethoxy) dihydroartemisinin was named AS I and AS with 12-(-1*H*-benzo [de] isoquinoline-1, 3(2*H*)-dione-2-ethoxy) dihydroartemisinin was named AS II. (g) Effect of V_{D3} (100 nM) on TNF-α levels in LPS-tolerant RAW264.7 cells treated with AS (n = 5). One-way ANOVA followed by Tukey's post hoc test; ns, not significant; $^{*}P < 0.05$

artesunate-induced TNF-α increase in LPS-tolerant cells was abrogated by overexpressing *Vdr* (Figure 3e). These findings suggested VDR as an essential and key molecule in LPS-tolerant formation and could be further considered as a candidate interactor for artesunate.

Third, to verify the interaction between artesunate and VDR, an indirect competitive binding assay using fluorophore-labelled artesunate was carried out (Figure 3f1). Pre-incubation with V_{D3} decreased the artesunate-related fluorescence intensity significantly (Figure 3f2), suggesting that V_{D3} occupied the receptor to decrease the interaction between artesunate and VDR.

Last, V_{D3} is a natural agonist that showed high affinity for VDR (Haussler, Jurutka, Mizwicki, & Norman, 2011),therefore the effect of artesunate on TNF-α level was determined in presence and in absence of V_{D3}. In the absence of V_{D3}, the TNF-α level decreased and

artesunate increased TNF-α release from LPS-tolerant cells. However, after pre-incubation with V_{D3}, artesunate-induced TNF-α increase was eliminated (Figure 3g), indicating antagonism between V_{D3} and artesunate. These results strongly indicated that artesunate binds to the same receptor and even similar sites, as V_{D3}.

These findings demonstrated that artesunate interacts with VDR and inhibits its biological function. Therefore, we considered that artesunate might interact with VDR as an antagonist to reverse the LPS-tolerant state.

3.4 | Artesunate inhibits the nuclear translocation of VDR and modulates the transcription of its target gene, *Atg16l1*

VDR is a nuclear receptor that mediates most of the biological functions of V_{D3} and translocate into the nucleus to regulate the transcription of downstream target genes, such as *Atg16l1* by binding to their promotors (Baeke, Gysemans, Korf, & Mathieu, 2010), thus regulating V_{D3}-mediated regulation of autophagy and antibacterial effects (Sun, 2016). Therefore, we investigated the nuclear translocation of VDR and its subsequent effect on autophagy related 16 like 1 (ATG16L1) first. Immunoblotting and immunostaining showed that the VDR protein level increased dramatically in the nucleus of LPS-tolerant cells compared with LPS cells, which could be reversed by artesunate (Figure 4a,b). Second, ChIP assay results showed that artesunate induced binding of VDR to the *Atg16l1* promoter, as analysed using semiquantitative PCR and RT-PCR in LPS-tolerant cells (Figure 4c,d). Together, these data showed that artesunate's effect is associated with transcriptional regulation by VDR on *Atg16l1*. Third, immunoblotting indicated that the level of ATG16L1 in LPS-tolerant cells decreased markedly compared with that in LPS cells, but artesunate increased its level (Figure 4e), which did not change in presence of V_{D3} (Figure S3a,b). The results suggested that VDR regulates *Atg16l1* transcription negatively in LPS-tolerant cells, which could be prevented by artesunate. Additionally, the level of ATG16L1 in LPS-tolerant cells markedly increased in the *Vdr*-KD group compared with that in NC-KD group and the effect of artesunate was diminished (Figure 4f). However, the artesunate-induced increase in ATG16L1 levels in LPS-tolerant cells was abrogated by overexpression of *Vdr* (Figure 4g). These findings indicated that artesunate inhibits the function of VDR via preventing the nuclear translocation of VDR, thus influencing the transcription of its target gene *Atg16l1*.

3.5 | Artesunate's autophagy-dependent effects act through VDR *in vitro*

Autophagy is an important self-protection mechanism required for bacterial clearance and inflammation (Gutierrez et al., 2004; Levine, Mizushima, & Virgin, 2011). *Atg16l1*, the target gene of VDR and an autophagy regulator, links VDR and autophagy (Wu & Sun, 2011). First, to confirm the function of ATG16L1, cells were treated with *Atg16l1* siRNA (Figure S4a). TNF-α and IL-6 levels in LPS cells decreased and artesunate-induced TNF-α and IL-6 increase in LPS-tolerant cells were eliminated in the *Atg16l1* siRNA-infected group compared with those in the negative control group (Figures 5a and S4a). This suggested that ATG16L1 is associated with inflammatory cytokine release in LPS-tolerant cells and in the effects of artesunate.

Second, three autophagy inhibitors, 3-MA targeting Vps34; Bafilomycin A1 blocking autophagosome and lysosome fusion; and LY294002 targeting Vps34 (also known as PI3K catalytic subunit type 3), were used in RAW264.7 cells. TNF-α and IL-6 levels in LPS cells decreased and artesunate-induced TNF-α and IL-6 increase in LPS-tolerant cells were significantly eliminated after pre-incubation with bafilomycin A1 (Figure 5b) and 3-MA (Figure 5c). Furthermore, artesunate markedly reduced the bacterial load in LPS-tolerant cells challenged with *Pseudomonas aeruginosa* and this effect was abrogated by pre-incubation with 3-MA, LY294002, or bafilomycin A1 (Figure 5d). These results indicated a potential correlation between autophagy and the effect of artesunate.

Third, the influence of artesunate on autophagy-related molecules was further investigated. Markers such as the conversion of microtubule associated protein 1 light chain 3 (LC3B-I) (18 kDa) to LC3B-II (16 kDa) and the accumulation of autophagy related 5 (ATG5) were selected to evaluate autophagy activity (Schaaf, Keulers, Vooijs, & Rouschop, 2016). LPS treatment increased LC3B-II and ATG5 levels dose-dependently (Figure 5e1), which was consistent with the results that LPS induced pro-inflammatory cytokines release in a dose-dependent manner (Figure 2a). This further suggested that LPS-induced cytokine release is autophagy involved. Immunoblotting showed that LC3B-II and ATG5 levels changed with time in LPS-tolerant cells and peaked at 1 h (Figure 5e2), which was selected as the best time point to observe LPS-induced autophagic activities.

Fourth, immunofluorescence staining, transmission electron microscopy (TEM) and immunoblotting results revealed that autophagy was remarkably decreased in LPS-tolerant cells relative to LPS cells and could be reversed by artesunate treatment (Figures S4b, 5f and 5g). These results indicated that autophagy decline is associated with the LPS-tolerant phenotype and artesunate treatment potentiated autophagic activities.

Last, in LPS-tolerant cells, LC3B-II and ATG5 levels increased markedly in *Vdr*-KD group compared with that in the negative control and artesunate addition had no effect (Figure 5h). artesunate-induced LC3B-II and ATG5 increase in LPS-tolerant cells was abrogated by overexpressing *Vdr* (Figure 5i). These findings indicated that artesunate's autophagy-dependent effects act through VDR *in vitro*.

3.6 | Artesunate inhibits the interaction between VDR and NF-κB p65 *in vitro*

Transcription factor NF-κB regulates the transcription of many pro-inflammatory cytokines including TNF-α and IL-6 (Bonizzi & Karin, 2004). VDR physically interacts with NF-κB p65 in mouse embryonic fibroblast cells and intestinal cells (Sun et al., 2006; Wu

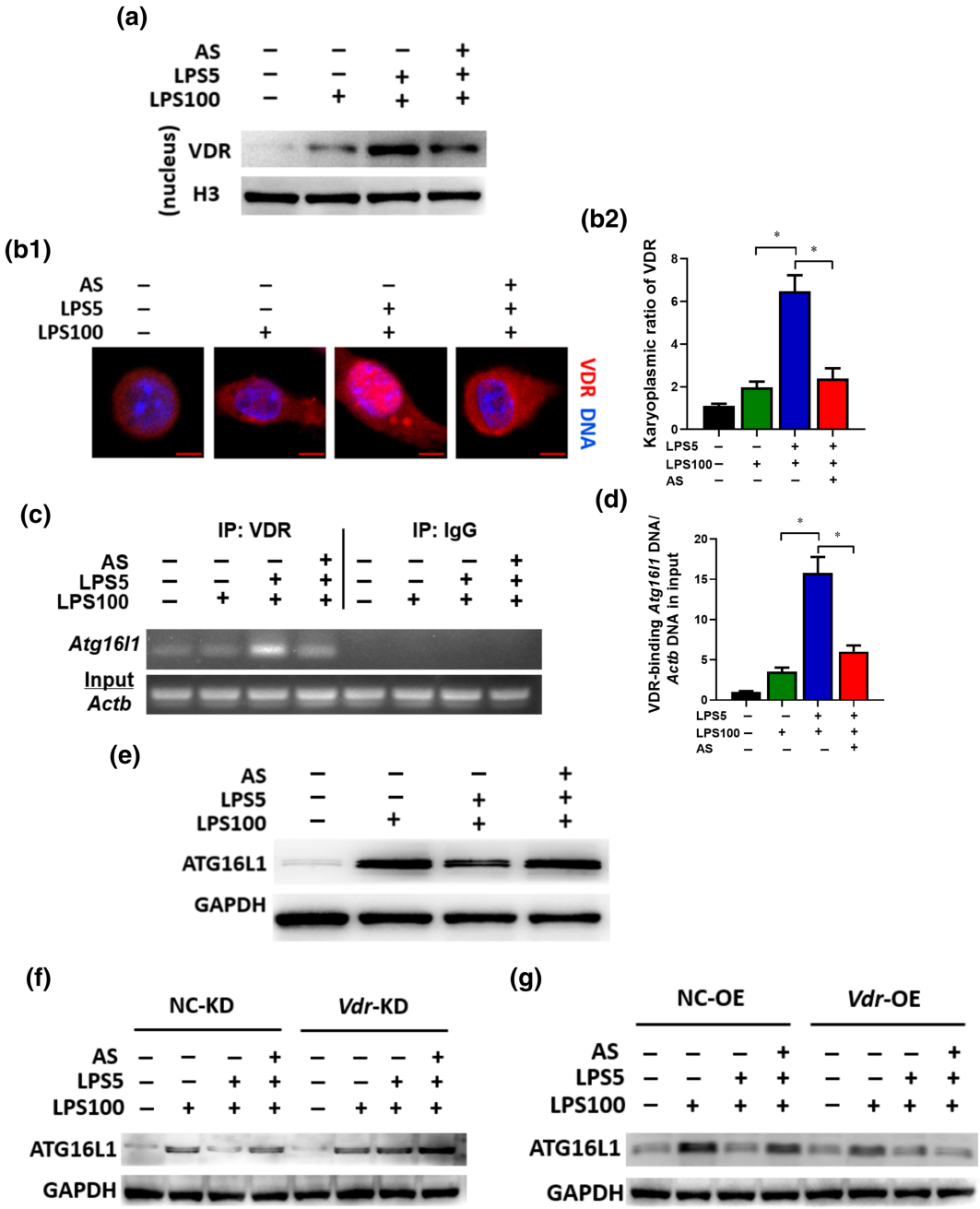

FIGURE 4 Artesunate (AS) inhibits the nuclear translocation of VDR and modulates the transcription of its target gene *Atg16l1*. RAW264.7 cells were treated as described in the legend of Figure 2d. (a) Immunoblotting to observe the VDR level in the nuclear lysate. (b) Immunostaining to observe the nuclear translocation of VDR. VDR was probed using Alexa Fluor 555 (red). Representative images (bar = 5 μm) (b1). The karyoplasmic ratio of VDR was quantified from 100 cells (normalized to medium) (b2). (c) ChIP analysis for the binding of VDR to the *Atg16l1* promoter. The protein–DNA complex was immunoprecipitated with anti-VDR antibody or a negative control IgG. Representative agarose gels for the VDR-binding region in the *Atg16l1* promoter and *Actb* DNA in the input amplified using semiquantitative PCR. (d) The binding of VDR to the *Atg16l1* promoter, normalized to *Actb* DNA in the input, analysed by qPCR ($n = 5$). (e) The protein level of ATG16L1 in LPS-tolerant RAW264.7 cells treated with AS. (f) Change in ATG16L1 protein levels in LPS-tolerant RAW264.7 cells (*Vdr*-KD) treated with AS. (g) Change in ATG16L1 protein levels in *Vdr*-OE LPS-tolerant RAW264.7 cells treated with AS. One-way ANOVA followed by Tukey's post hoc test; $^{*}P < 0.05$

et al., 2010); the functional relevance of this interaction in LPS-tolerant macrophages remains unclear. Co-IP and fluorescent co-localization experiments were performed, which showed that the associated NF-κB p65 level in the cytoplasm showed no significant change in the medium cells, LPS cells and LPS-tolerant cells when an equal amount of VDR was used as a control (pull-down by VDR); the NF-κB p65 level was significantly decreased by artesunate treatment (Figure 6a1). However, artesunate had no effect on the associated

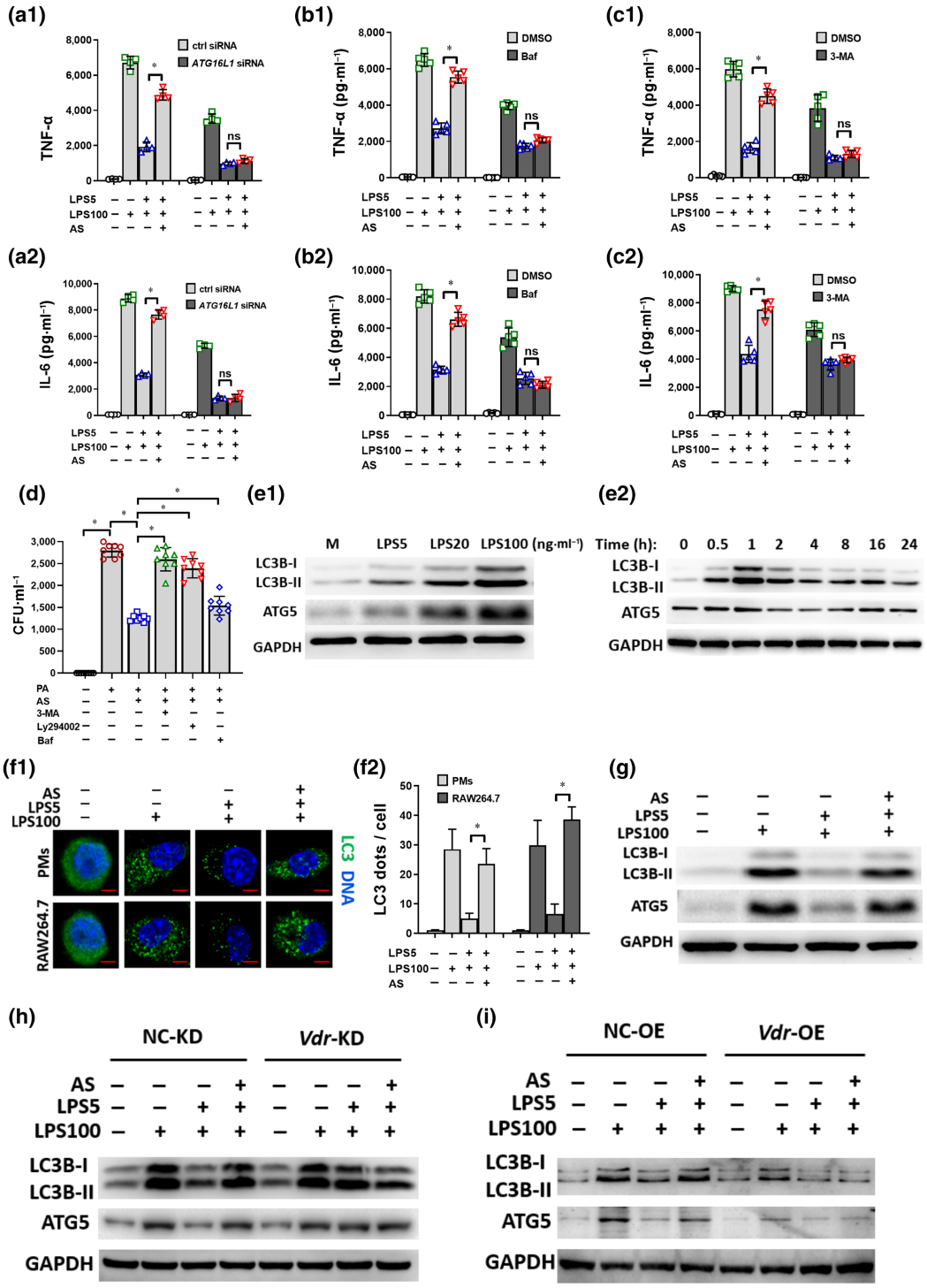

FIGURE 5 Artesunate's (AS) effect is autophagy-dependent through VDR in vitro. (a) Effect of *Atg16l1* siRNA on TNF-α (a1) and IL-6 (a2) levels in LPS-tolerant RAW264.7 cells treated with AS (n = 5). (b) Effect of bafilomycin (Baf) (10 ng·ml^{-1}) on TNF-α (b1) and IL-6 (b1) levels in LPS-tolerant RAW264.7 cells treated with AS (n = 5). (c) Effect of 3-MA (5 mM) on TNF-α (c1) and IL-6 (c2) levels in LPS-tolerant RAW264.7 cells treated with AS (n = 5). (d) Effect of 3-MA, Ly294002 (10 μM), or Baf on the bacterial clearance in LPS-tolerant RAW264.7 cells treated with AS (n = 8). (e1) LPS increased the protein levels of LC3B-I, LC3B-II and ATG5 in a dose-dependent manner in RAW264.7 cells. (e2) The protein levels of LC3B-I, LC3B-II and ATG5 over time in RAW264.7 cells treated with LPS (100 ng·ml^{-1}). The level of expression peaked at 1 h. (f) Representative image of immunofluorescence staining of LC3B in LPS-tolerant RAW264.7 cells treated with AS (bar = 2 μm). (f1) Relative fluorescent puncta indicating LC3B aggregation were quantified from 100 cells; the number in the medium group was normalized as 1 (f2). (g) The protein levels of LC3B-II, ATG16L1 and ATG5 in LPS-tolerant RAW264.7 cells treated with AS. (h) Changes in LC3B-II, ATG16L1 and ATG5 protein levels in LPS-tolerant RAW264.7 cells (*Vdr*-KD) treated with AS. (i) Changes in LC3B-II, ATG16L1 and ATG5 protein levels in LPS-tolerant RAW264.7 cells (*Vdr*-OE) treated with AS. One-way ANOVA followed by Tukey's post hoc test; ns, not significant; $^{*}P < 0.05$

NF-κB p65 protein in the nucleus in any treatment in which an equal amount of VDR was used as a control (pull-down by VDR) (Figure 6a2). Thus, artesunate might bind VDR to interrupt its interaction with NF-κB p65 in the cytoplasm, further implying that artesunate affects NF-κB p65 activity.

Subsequently, immunostaining was used to determine whether artesunate affected the intracellular co-localization and distribution of VDR and NF-κB p65. Co-localization of VDR and NF-κB p65 was observed in LPS-tolerant cells, which was significantly inhibited by artesunate (Figure 6b1,b2). Moreover, NF-κB p65 nuclear translocation declined markedly in LPS-tolerant cells relative to LPS cells, which was reversed by artesunate treatment (Figure 6b1,b3). These results indicated that high levels of VDR interacted with NF-κB p65 to prevent its nuclear translocation. Notably, artesunate inhibited the

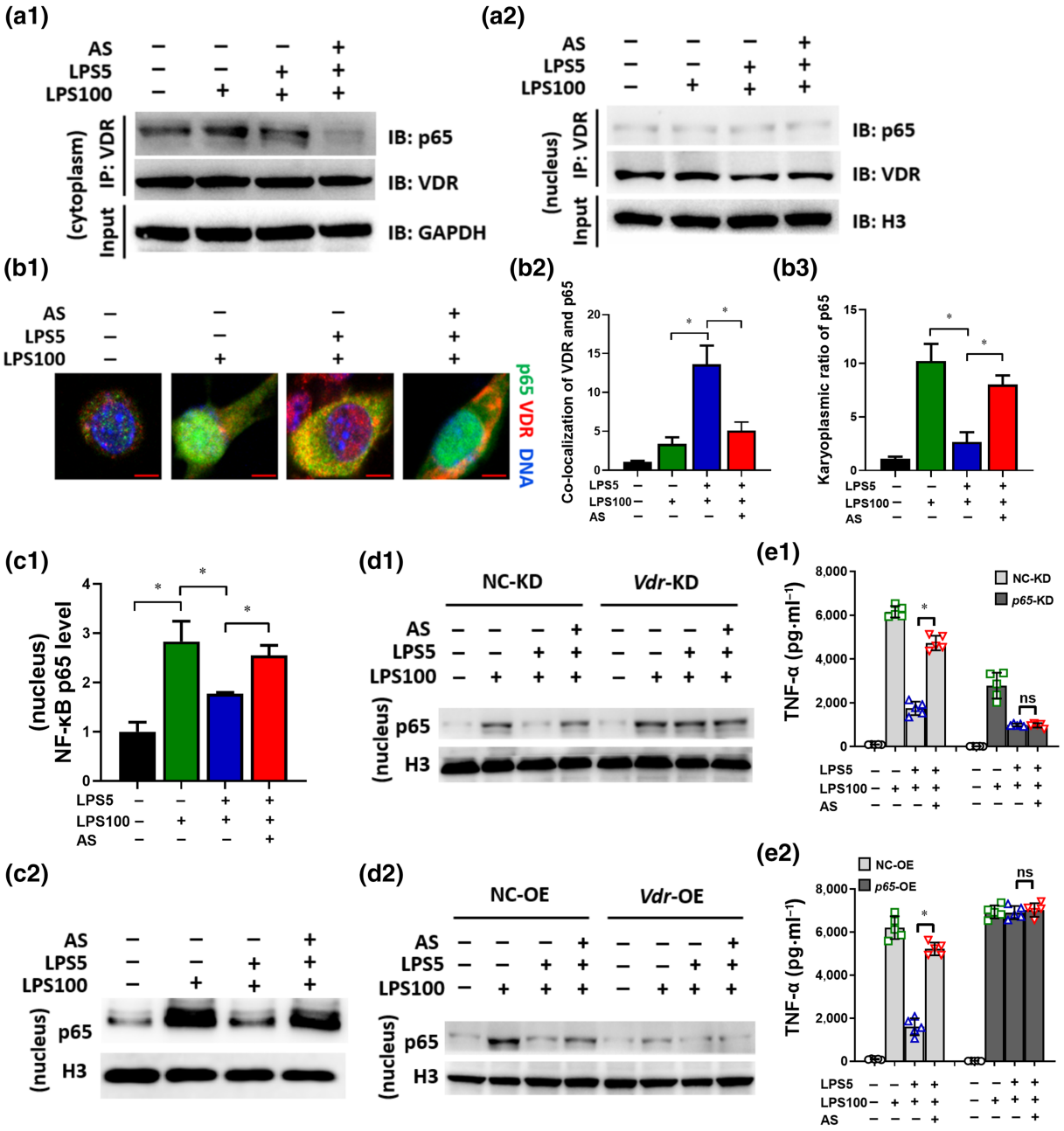

FIGURE 6 Artesunate (AS) inhibits the physical interaction between VDR and NF-κB p65 in LPS-tolerant macrophages. RAW264.7 cells were treated as described in the legend of Figure 2d. (a) The cytoplasm (a1) and nuclear (a2) lysate were used for an IP experiment using anti-VDR antibodies and the associated NF-κB p65 (p65) was detected by immunoblotting (IB). (b) Immunostaining to observe the co-localization of p65 and VDR. p65 was probed using Alexa Fluor 488 (green). VDR was probed using Alexa Fluor 555 (red). Representative images are shown (bar = 5 μm) (b1). The co-localization of VDR and p65 (b2) and the karyoplasmic ratio of p65 (b3) was quantified from 100 cells (normalized to medium). (c) The p65 level in the nuclear lysate was detected using ELISA and WB. (d) Change in the p65 level in *Vdr*-KD (d1) or *Vdr*-OE (d2) LPS-tolerant RAW264.7 cells treated with AS. (e) Change in the TNF-α level in *p65*-KD (e1) or *p65*-OE (e2) LPS-tolerant RAW264.7 cells treated with AS (n = 5). One-way ANOVA followed by Tukey's post hoc test; ns, not significant; $^{*}P < 0.05$

interaction between VDR and NF-κB p65, accelerating NF-κB p65 nuclear translocation. For confirmation, the nuclear protein level of NF-κB p65 was investigated using ELISA and immunoblotting, which showed that nuclear NF-κB p65 levels decreased markedly in LPS-tolerant cells relative to LPS cells, which was reversed by artesunate (Figure 6c1,c2). In LPS-tolerant cells, the nuclear NF-κB p65 level increased in the *Vdr*-KD group compared with that in the negative control, leading to a loss of the tolerant phenotype (Figure 6d1). In *Vdr*-OE cells, the nuclear NF-κB p65 level decreased markedly suppressed compared with that in the negative control and artesunate treatment had no effect in LPS-tolerant cells (Figure 6d2). To determine whether artesunate-induced pro-inflammatory cytokines release in LPS-tolerant cells is related to its influence on NF-κB p65 activity, NF-κB p65 expression in RAW264.7 was modified (Figure S5a,b). Knockdown of NF-κB p65 reduced pro-inflammatory cytokine release and abrogated artesunate's effect (Figure 6e1). Overexpression of NF-κB p65 led to loss of the LPS-tolerant phenotype and artesunate addition had no effect (Figure 6e2). These findings indicated that artesunate inhibited the physical interaction between VDR and NF-κB p65 in LPS-tolerant macrophages, promoting NF-κB p65 nuclear translocation and downstream pro-inflammatory cytokine release.

3.7 | Knockdown of *Vdr* results in the loss of the effect of artesunate *in vivo*

To verify the *in vitro* findings, the mRNA and protein levels of *Vdr* were measured in CLP mice. The levels of *Vdr* mRNA and protein significantly increased in peritoneal macrophages of CLP mice but were markedly inhibited by artesunate (Figure 7a), which was consistent with the in vitro results. In *Vdr*-KD CLP mice, in which *Vdr* expression was knocked down using a lentiviral vector harbouring a *Vdr* RNAi sequence (*Vdr*-KD) (Figure S6a,b), TNF-α levels in the spleen and lungs increased significantly compared with those in the negative control and artesunate administration had no effect (Figure 7b). This suggested that *Vdr* overexpression is involved in sepsis-induced immunosuppression formation and knockdown of *Vdr* would lead to a loss of the immunosuppressive phenotype. Immunoblotting results showed that autophagy-associated protein levels in the spleen of CLP mice were increased compared with those in the negative control and artesunate treatment had no effect (Figure 7c). Taken together, the *in vivo* and *in vitro* results indicated that the VDR plays an important role in sepsis-induced immunosuppression and the effects of artesunate.

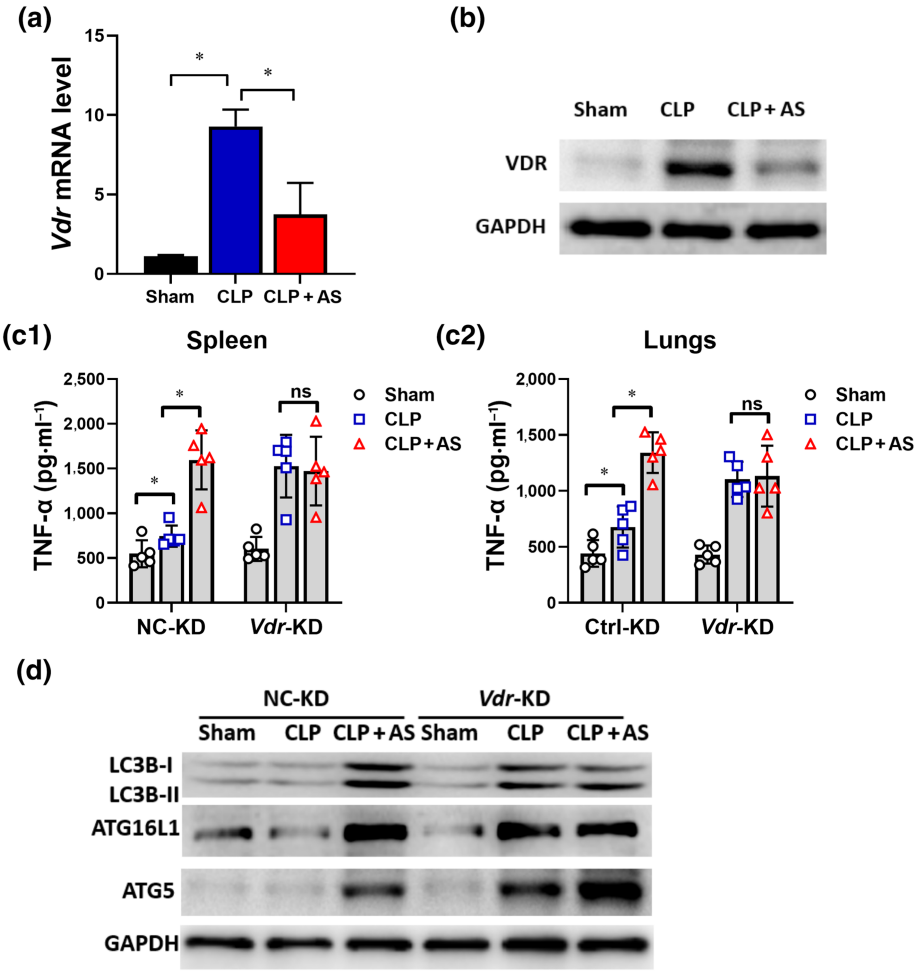

FIGURE 7 Knockdown of *Vdr* results in the loss of the effect of artesunate (AS) *in vivo*. (a) Effect of AS on the *Vdr* mRNA level of peritoneal macrophages (PMs) from caecal ligation and puncture (CLP) mice (n = 5). (b) Effect of AS on the VDR protein level of PMs from CLP mice. (c) Change in the effect of AS on the level of TNF-α and IL-6 in the spleen (c1) and lungs (c2) from *Vdr*-KD mice (n = 5). (d) Changes in the levels of LC3B-I, LC3B-II, ATG16L and ATG5 protein levels in the spleens of *Vdr*-KD mice. One-way ANOVA followed by Tukey's post hoc test; ns, non-significant; $^{*}P < 0.05$

4 | DISCUSSION

Our results demonstrated that artesunate interacts with vitamin D receptor (VDR; nuclear receptor subfamily 1 group I member 1, NR1I1) to reverse sepsis-induced immunosuppression in an autophagy and NF-κB-dependent manner. Together with our previous results (Kuang et al., 2018; Li et al., 2008), artesunate not only inhibits pro-inflammatory cytokine release during the hyper-inflammation stage but also enhances pro-inflammatory cytokine release and bacterial clearance by macrophages, thus reversing sepsis-induced immunosuppression in vivo and in vitro, demonstrating that artesunate exhibits a bidirectional immunoregulating effect for sepsis treatment, which is not reported previously.

Sepsis is a life-threatening condition caused by a dysregulated host response to infection such as bacterial, fungal, viral and parasitic infection (Singer et al., 2016). Recently, reversing sepsis-induced immunosuppression has become the focus of sepsis research, instead of targeting the cytokine storm (Cohen, 2002; Hotchkiss et al., 2013a; Kox et al., 2000; Prucha et al., 2017). However, drugs in current clinical trials, such as anti-programmed cell death receptor-1 (anti-PD-1) and anti-PD-L1 antibodies, might only affect the immunosuppression stage (Hotchkiss et al., 2013a; Prucha et al., 2017) and their clinical efficacies remain to be proven. Therefore, we consider that an ideal immunotherapy for sepsis should exert an anti-inflammatory effect during the cytokine storm stage and increase the resistance to infection during the immunosuppression stage. The therapeutic effects of artesunate on the cytokine storm stage and its possible mechanism have been proved in our previous study (Kuang et al., 2018; Li et al., 2008; Li et al., 2010). The results of the present study revealed artesunate's additional therapeutic effects in sepsis-induced immunosuppression *in vivo* and *in vitro*.

Active VDR binds preferentially as a heterodimer with the **retinoid X receptor** (RXR) to hexameric repeats on vitamin D response elements in the promoter regions of target genes (Haussler et al., 1998; Orlov, Rochel, Moras, & Klaholz, 2012). VDR/RXR heterodimer nuclear translocation functions to recruit additional cofactors that play an essential role in transcription (Haussler et al., 1998). Thus, TCMSP predicted VDR as an artesunate interacting molecule and was then identified using PCR and western blotting. Moreover, we found that in LPS-tolerant cells (mimicking the immunosuppression stage of sepsis), VDR was highly expressed and its nuclear translocation increased compared with that in LPS cells (mimicking the cytokines storm stage), while artesunate treatment markedly inhibited VDR expression and nuclear translocation. Furthermore, the artesunate–VDR interaction was confirmed using binding assays. Thus, artesunate might interact with VDR to inactivate it, thereby inhibiting its nuclear translocation. The effects of artesunate were investigated in presence and in absence of V_{D3}, the natural ligand of VDR. artesunate's effect was eliminated when pre-incubated with V_{D3}, demonstrating antagonism between V_{D3} and artesunate, suggesting that artesunate might bind to the same receptor even similar sites as V_{D3}.

Although the anti-inflammation or immunosuppressive effect of V_{D3} is tightly related to VDR function (Alroy, Towers, & Freedman, 1995; Joshi et al., 2011; Lemire et al., 1985), few studies have addressed the direct role of VDR in sepsis-induced immunosuppression. Our results demonstrated that the excessive high levels of VDR during the immunosuppression stage of sepsis might be related to the decreased inflammatory response. Indeed, artesunate increased the survival rate of septic animals by inhibiting the excessive high expression of VDR.

Autophagy participates in the defence against infection by eliminating intracellular pathogens and regulating inflammation (Casanova, 2017). Autophagy has been considered a new target in sepsis treatment (Ren et al., 2017). Combined with our previous study (Kuang et al., 2018), we considered that autophagy was enhanced in early sepsis stage (cytokine storm stage) but suppressed in late sepsis (immunosuppression stage). Our results showed artesunate enhanced autophagy in LPS-tolerant cells to eliminate bacteria. Inhibiting autophagy using *Atg16l1* siRNA or autophagy inhibitors abrogated artesunate's effects on bacteria clearance and cytokine releases, demonstrating that autophagy plays a crucial part in artesunate's effect.

VDR is involved in immunoregulation and resistance to infections via regulating autophagy (Baeke, Takiishi, Korf, Gysemans, & Mathieu, 2010; Gois, Ferreira, Olenski, & Seguro, 2017). VDR transcriptionally regulates *Atg16l1*, which is an important autophagy-related protein. Decreased VDR reduces ATG16L1 levels associated with abnormal Paneth cells in chronic states of mucosal inflammation (Sun, 2016). However, we observed tight binding between VDR and *Atg16l1* promotor, leading to low ATG16L1 protein levels in LPS-tolerant cells, demonstrating negative regulation by VDR on *Atg16l1* transcription in LPS-tolerant cells, which did not change in presence of V_{D3}. Most effects of VDR on ATG16L1 and autophagy were investigated in epithelial cells (Huang, 2016; Sun, 2016) but not in monocytes/macrophages. Our study focused on the immunosuppression stage in monocytes/macrophages, unlike the parenchyma cells such as epithelial cells which were not immunosuppressed. Thus, there might be differences between two different kinds of cells. Moreover, considering that artesunate inhibited VDR expression to up-regulate *Atg16l1* transcription and increase autophagy, we speculated that the discrepancy in the transcriptional regulation between VDR and *Atg16l1* might due to the differences in the inflammation and immune status, which will require further investigation in the future.

The NF-κB signalling pathway links pathogenic and cellular danger signals, thus organizing cellular resistance to invading pathogens and forming a network hub responsible for complex biological signalling (Albensi & Mattson, 2000; Kaltschmidt & Kaltschmidt, 2009). NF-κB p65 physically interacts with VDR in mouse embryonic fibroblast cells and intestinal cells (Sun et al., 2006; Wu et al., 2010). Previously, we showed that artesunate significantly inhibited LPS-induced toll-like receptor 4 (**TLR4**)/TRAF6/NF-κB activation in macrophages, reducing pro-inflammatory cytokine release (Kuang et al., 2018; Li et al., 2008) and thus playing an anti-inflammatory role. Herein, we focused on its function in sepsis immunosuppression and have shown that VDR negatively regulates NF-κB p65 via their physical interaction in macrophages. Importantly, artesunate disrupted the VDR–NF-κB p65 interaction in LPS-tolerant cells, markedly increasing nuclear NF-κB p65 translocation and downstream target gene expression, such as

TNF-α and IL-6. Furthermore, artesunate decreased VDR binding to the promoter of *Atg16l1*, leading to reduced VDR nuclear translocation and decreasing the negative transcription of *Atg16l1*. Lastly, artesunate enhanced autophagy activities through binding to VDR. In the immunosuppression stage, *Vdr* knockdown reversed autophagy-related protein levels and *Vdr* overexpression resulted in the loss of artesunate-induced autophagy-related protein increase. Thus, artesunate's interaction with VDR to reverse immunosuppression involves autophagy. We speculated that artesunate interacts with VDR to inhibit nuclear translocation of VDR and inhibited the interaction between VDR and NF-κB p65 in LPS-tolerant macrophages. This would promote NF-κB p65 nuclear translocation, enhance autophagy and activate NF-κB p65 target gene transcription, such as pro-inflammatory cytokine genes.

VDR is the receptor for V_{D3}. Does V_{D3} control VDR to achieve an anti-sepsis effect? Although clinical investigation have shown a close correlation between vitamin D deficiency in serum and excess morbidity and mortality of sepsis, suggesting that vitamin D deficiency is closely related to sepsis (Dickerson et al., 2016), it remains conflicting whether vitamin D supplementation improves the outcome of patients with sepsis (Kearns, Alvarez, Seidel, & Tangpricha, 2015; Putzu et al., 2017). The extensive biological effects of vitamin D and its role in homeostasis maintenance require a maintained physiological concentration of vitamin D. Noteworthily, based on our results that excessive vitamin D induces increases VDR expression and subsequent suppressed immune function, excessive vitamin D supplementation might be harmful rather than beneficial.

To date, the outcome of therapy only aimed at a single stage of sepsis has been disappointing, possibly because the treatment time window is important for the therapeutic regimen of sepsis, but difficult to handle. Anti-inflammatory treatment in the hypo-inflammatory stage or pro-inflammatory therapy in the hyper-inflammatory stage failed or even increased mortality in clinic (Hotchkiss et al., 2013a; Rudick, Cornell, & Agrawal, 2017). Therefore, we considered that an immunoregulator might be an ideal drug to treat sepsis caused by bacterial or virus without limitation of treatment time. Based on our previous and present results, artesunate might be a bidirectional immunoregulator for both the hyper- and hypo-inflammatory stages of sepsis even caused by COVID-19.

Mechanistically, artesunate exerts its "pro-inflammatory" effect in the immunosuppression stage in contrast to its "anti-inflammatory" effect in the cytokines storm stage. Our present results showed a schematic of the mechanism of artesunate's effect through two ways:- artesunate interacts with VDR, to preventing its nuclear translocation of VDR, which decreases its negative regulation of autophagy-related target genes, such as *Atg16l1*, and increases autophagy. Additionally, artesunate interaction with VDR prevents the VDR–NF-κB p65 interaction, promoting the nuclear translocation of NF-κB p65, leading to increased transcription of its target genes, such as pro-inflammatory cytokines (Figure 8). These two actions increase bacterial clearance and pro-inflammatory cytokine release from macrophages.

Although the monocytes/macrophages system plays a vital role in sepsis, the acquired immune system is equally important. However, the effect of artesunate on T and B cell function remains to be investigated. Considering the therapeutic effect of artesunate on caecal ligation and puncture (CLP) mouse models, we believe that artesunate could improve T and B cells function during sepsis. Artesunate interacts with VDR, however more work is required to determine whether VDR is a target of artesunate. Overall, our findings provide evidence

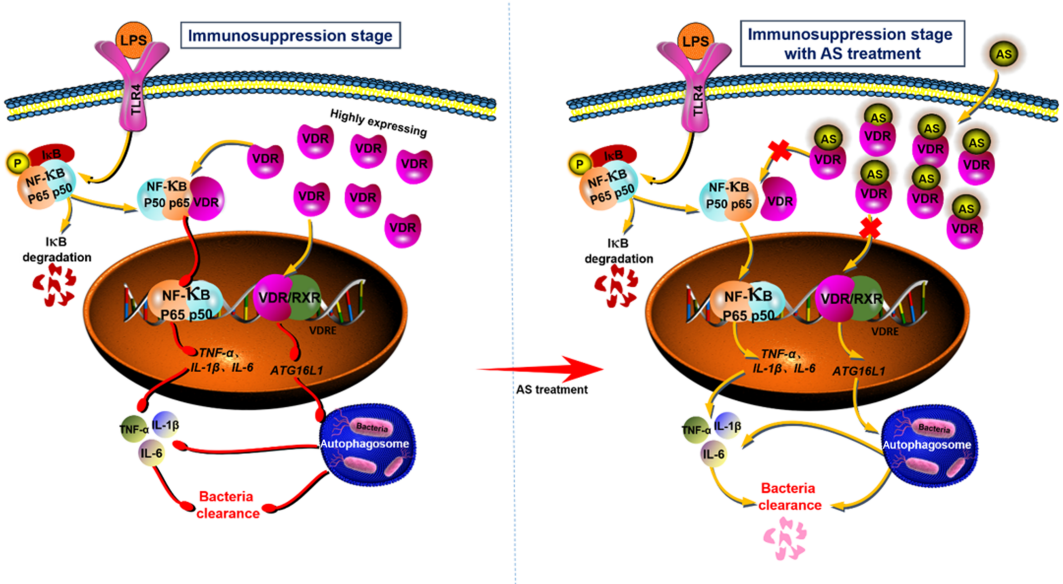

FIGURE 8 Flow chart of the mechanism of action of artesunate (AS). AS interacts with vitamin D receptor (VDR) to prevent the nuclear translocation of VDR and decrease its negative regulation of autophagy-related target genes such as *Atg16l1*, which increases autophagy activity. Additionally, AS interacts with VDR to prevent the interaction between VDR and NF-κB p65, which increases the nuclear translocation of NF-κB p65, leading to increased transcription of its target genes, such as pro-inflammatory cytokines

that artesunate interacts with VDR to reverse sepsis-induced immunosuppression in an autophagy and NF-κB-dependent manner, highlighting a novel approach for the treatment of sepsis and the drug repurposing of artesunate as a bidirectional immunomodulator.

ACKNOWLEDGEMENTS

This work was supported by grants from the National Natural Science Foundation of China (grant numbers 81872914, 81772137 and 81673495), Major National Science and Technology Program of China for Innovative Drug (2017ZX09101002-002-009) and the fourth batch of "Thousand People Innovation and Entrepreneurship Talents Fund" in Guizhou Province, Shijingshan's Tutor Studio of Pharmacology. We sincerely thank Qin Ouyang for his meaningful advice regarding drug targets, Prof. Qiaonan Guo for her electron microscopy assistance and all members of the Zheng laboratory for their help and support. We sincerely thank Dongmei Deng, Bin Li, Mei Kuang, Rongxin Qin, Xichun Pan, Yanyan Cen, Chao Liu, Xiaoli Chen, Zhaoxia Zhai, Yongling Lu and Yan Wang from the Third Military Medical University. We also sincerely thank Huang Chao and Xuetong Chen from the Northwest University for their assistance in this study.

AUTHOR CONTRIBUTIONS

S.S., J.W. and X.L. performed the study under the guidance of H.Z. and S.S. collected and analysed the data. H.Z. and S.S. wrote the manuscript. X.L. and P.L. contributed to establishing the mouse models. S.S. and L.X. performed the bacteria clearance experiments. S.S. and J.W. were responsible for the molecular biology experiments. Y.W. and X.C. completed the bioinformatics analysis. H.Z., J.Z., S.L. and S.S. contributed to discussions. H.Z., J.Z. and S.L. revised the manuscript. H.Z. is the guarantor of this work, has full access to all the data and takes full responsibility for the integrity of the data.

CONFLICT OF INTEREST

The authors declare no conflicts of interest.

DECLARATION OF TRANSPARENCY AND SCIENTIFIC RIGOUR

This Declaration acknowledges that this paper adheres to the principles for transparent reporting and scientific rigour of preclinical research as stated in the *BJP* guidelines for Design & Analysis, Immunoblotting and Immunochemistry, and Animal Experimentation and as recommended by funding agencies, publishers and other organizations engaged with supporting research.

REFERENCES

Albensi, B. C., & Mattson, M. P. (2000). Evidence for the involvement of TNF and NF-κB in hippocampal synaptic plasticity. *Synapse*, *35*, 151–159. https://doi.org/10.1002/(SICI)1098-2396(200002)35:2<151::AID-SYN8>3.0.CO;2-P

Alexander, S. P. H., Cidlowski, J. A., Kelly, E., Mathie, A., Peters, J. A., Veale, E. L., … CGTP Collaborators. (2019). The Concise Guide to PHARMACOLOGY 2019/20: Nuclear hormone receptors. *British Journal of Pharmacology*, *176*(Suppl 1), S229–S246.

Alexander, S. P. H., Roberts, R. E., Broughton, B. R. S., Sobey, C. G., George, C. H., Stanford, S. C., … Ahluwalia, A. (2018). Goals and practicalities of immunoblotting and immunohistochemistry: A guide for submission to the *British Journal of Pharmacology*. *British Journal of Pharmacology*, *175*, 407–411. https://doi.org/10.1111/bph.14112

Alroy, I., Towers, T. L., & Freedman, L. P. (1995). Transcriptional repression of the interleukin-2 gene by vitamin D3: Direct inhibition of NFATp/-AP-1 complex formation by a nuclear hormone receptor. *Molecular and Cellular Biology*, *15*, 5789–5799. https://doi.org/10.1128/MCB.15.10.5789

Angus, D. C., & van der Poll, T. (2013). Severe sepsis and septic shock. *The New England Journal of Medicine*, *369*, 840–851. https://doi.org/10.1056/NEJMra1208623

Baeke, F., Gysemans, C., Korf, H., & Mathieu, C. (2010). Vitamin D insufficiency: Implications for the immune system. *Pediatric Nephrology*, *25*, 1597–1606. https://doi.org/10.1007/s00467-010-1452-y

Baeke, F., Takiishi, T., Korf, H., Gysemans, C., & Mathieu, C. (2010). Vitamin D: Modulator of the immune system. *Current Opinion in Pharmacology*, *10*, 482–496. https://doi.org/10.1016/j.coph.2010.04.001

Bonizzi, G., & Karin, M. (2004). The two NF-κB activation pathways and their role in innate and adaptive immunity. *Trends in Immunology*, *25*, 280–288. https://doi.org/10.1016/j.it.2004.03.008

Bretin, A., Carriere, J., Dalmasso, G., Bergougnoux, A., B'Chir, W., Maurin, A. C., … Nguyen, H. T. T. (2016). Activation of the EIF2AK4-EIF2A/eIF2α-ATF4 pathway triggers autophagy response to Crohn disease-associated adherent-invasive *Escherichia coli* infection. *Autophagy*, *12*, 770–783. https://doi.org/10.1080/15548627.2016.1156823

Burrows, J. N., Chibale, K., & Wells, T. N. (2011). The state of the art in anti-malarial drug discovery and development. *Current Topics in Medicinal Chemistry*, *11*, 1226–1254. https://doi.org/10.2174/156802611795429194

Casanova, J. E. (2017). Bacterial autophagy: Offense and defense at the host-pathogen interface. *Cellular and Molecular Gastroenterology and Hepatology*, *4*, 237–243. https://doi.org/10.1016/j.jcmgh.2017.05.002

Clark, R. L., White, T. E., Clode, S. A., Gaunt, I., Winstanley, P., & Ward, S. A. (2004). Developmental toxicity of artesunate and an artesunate combination in the rat and rabbit. *Birth Defects Research. Part B, Developmental and Reproductive Toxicology*, *71*, 380–394. https://doi.org/10.1002/bdrb.20027

Cohen, J. (2002). The immunopathogenesis of sepsis. *Nature*, *420*, 885–891. https://doi.org/10.1038/nature01326

Curtis, M. J., Alexander, S., Cirino, G., Docherty, J. R., George, C. H., Giembycz, M. A., … Ahluwalia, A. (2018). Experimental design and analysis and their reporting II: Updated and simplified guidance for authors and peer reviewers. *British Journal of Pharmacology*, *175*, 987–993. https://doi.org/10.1111/bph.14153

Deng, D., Li, X., Liu, C., Zhai, Z., Li, B., Kuang, M., … Zhou, H. (2017). Systematic investigation on the turning point of over-inflammation to immunosuppression in CLP mice model and their characteristics. *International Immunopharmacology*, *42*, 49–58. https://doi.org/10.1016/j.intimp.2016.11.011

Dickerson, R. N., Van Cleve, J. R., Swanson, J. M., Maish, G. O. 3rd, Minard, G., Croce, M. A., & Brown, R. O. (2016). Vitamin D deficiency in critically ill patients with traumatic injuries. *Burns Trauma*, *4*, 28.

Efferth, T., Dunstan, H., Sauerbrey, A., Miyachi, H., & Chitambar, C. R. (2001). The anti-malarial artesunate is also active against cancer. *International Journal of Oncology*, *18*, 767–773.

Gois, P. H. F., Ferreira, D., Olenski, S., & Seguro, A. C. (2017). Vitamin D and infectious diseases: Simple bystander or contributing factor? *Nutrients*, *9*, 651. https://doi.org/10.3390/nu9070651

Gutierrez, M. G., Master, S. S., Singh, S. B., Taylor, G. A., Colombo, M. I., & Deretic, V. (2004). Autophagy is a defense mechanism inhibiting BCG

and *Mycobacterium tuberculosis* survival in infected macrophages. *Cell*, *119*, 753–766. https://doi.org/10.1016/j.cell.2004.11.038

Harding, S. D., Sharman, J. L., Faccenda, E., Southan, C., Pawson, A. J., Ireland, S., … NC-IUPHAR. (2018). The IUPHAR/BPS Guide to PHARMACOLOGY in 2018: Updates and expansion to encompass the new guide to IMMUNOPHARMACOLOGY. *Nucleic Acids Research*, *46*, D1091–D1106. https://doi.org/10.1093/nar/gkx1121

Haussler, M. R., Jurutka, P. W., Mizwicki, M., & Norman, A. W. (2011). Vitamin D receptor (VDR)-mediated actions of 1α,25(OH)$_2$vitamin D(3): Genomic and non-genomic mechanisms. *Best Practice & Research. Clinical Endocrinology & Metabolism*, *25*, 543–559. https://doi.org/10.1016/j.beem.2011.05.010

Haussler, M. R., Whitfield, G. K., Haussler, C. A., Hsieh, J. C., Thompson, P. D., Selznick, S. H., … Jurutka, P. W. (1998). The nuclear vitamin D receptor: Biological and molecular regulatory properties revealed. *Journal of Bone and Mineral Research*, *13*, 325–349. https://doi.org/10.1359/jbmr.1998.13.3.325

Ho, J., Yu, J., Wong, S. H., Zhang, L., Liu, X. D., Wong, W. T., … Wu, W. K. K. (2016). Autophagy in sepsis: Degradation into exhaustion? *Autophagy*, *12*, 1073–1082. https://doi.org/10.1080/15548627.2016.1179410

Hotchkiss, R. S., Monneret, G., & Payen, D. (2013a). Immunosuppression in sepsis: A novel understanding of the disorder and a new therapeutic approach. *The Lancet Infectious Diseases*, *13*, 260–268. https://doi.org/10.1016/S1473-3099(13)70001-X

Hotchkiss, R. S., Monneret, G., & Payen, D. (2013b). Sepsis-induced immunosuppression: From cellular dysfunctions to immunotherapy. *Nature Reviews. Immunology*, *13*, 862–874. https://doi.org/10.1038/nri3552

Huang, F. C. (2016). Vitamin D differentially regulates *Salmonella*-induced intestine epithelial autophagy and interleukin-1β expression. *World Journal of Gastroenterology*, *22*, 10353–10363. https://doi.org/10.3748/wjg.v22.i47.10353

Hutchins, N. A., Unsinger, J., Hotchkiss, R. S., & Ayala, A. (2014). The new normal: Immunomodulatory agents against sepsis immune suppression. *Trends in Molecular Medicine*, *20*, 224–233. https://doi.org/10.1016/j.molmed.2014.01.002

Joshi, S., Pantalena, L. C., Liu, X. K., Gaffen, S. L., Liu, H., Rohowsky-Kochan, C., … Youssef, S. (2011). 1,25-Dihydroxyvitamin D_3 ameliorates Th17 autoimmunity via transcriptional modulation of interleukin-17A. *Molecular and Cellular Biology*, *31*, 3653–3669. https://doi.org/10.1128/MCB.05020-11

Kaltschmidt, B., & Kaltschmidt, C. (2009). NF-κB in the nervous system. *Cold Spring Harbor Perspectives in Biology*, *1*, a001271.

Kearns, M. D., Alvarez, J. A., Seidel, N., & Tangpricha, V. (2015). Impact of vitamin D on infectious disease. *The American Journal of the Medical Sciences*, *349*, 245–262. https://doi.org/10.1097/MAJ.0000000000000360

Kilkenny, C., Browne, W., Cuthill, I. C., Emerson, M., Altman, D. G., & Group NCRRGW. (2010). Animal research: Reporting in vivo experiments: The ARRIVE guidelines. *British Journal of Pharmacology*, *160*, 1577–1579.

Kox, W. J., Volk, T., Kox, S. N., & Volk, H. D. (2000). Immunomodulatory therapies in sepsis. *Intensive Care Medicine*, *26*(Suppl 1), S124–S128. https://doi.org/10.1007/s001340051129

Kuang, M., Cen, Y., Qin, R., Shang, S., Zhai, Z., Liu, C., … Zhou, H. (2018). Artesunate attenuates pro-inflammatory cytokine release from macrophages by inhibiting TLR4-mediated autophagic activation via the TRAF6-Beclin1-PI3KC3 pathway. *Cellular Physiology and Biochemistry*, *47*, 475–488. https://doi.org/10.1159/000489982

Lemire, J. M., Adams, J. S., Kermani-Arab, V., Bakke, A. C., Sakai, R., & Jordan, S. C. (1985). 1,25-Dihydroxyvitamin D3 suppresses human T helper/inducer lymphocyte activity in vitro. *Journal of Immunology*, *134*, 3032–3035.

Levine, B., Mizushima, N., & Virgin, H. W. (2011). Autophagy in immunity and inflammation. *Nature*, *469*, 323–335. https://doi.org/10.1038/nature09782

Li, B., Li, J., Pan, X., Ding, G., Cao, H., Jiang, W., … Zhou, H. (2010). Artesunate protects sepsis model mice challenged with *Staphylococcus aureus* by decreasing TNF-α release via inhibition TLR2 and Nod2 mRNA expressions and transcription factor NF-κB activation. *International Immunopharmacology*, *10*, 344–350. https://doi.org/10.1016/j.intimp.2009.12.006

Li, B., Zhang, R., Li, J., Zhang, L., Ding, G., Luo, P., … Zhou, H. (2008). Antimalarial artesunate protects sepsis model mice against heat-killed *Escherichia coli* challenge by decreasing TLR4, TLR9 mRNA expressions and transcription factor NF-κB activation. *International Immunopharmacology*, *8*, 379–389. https://doi.org/10.1016/j.intimp.2007.10.024

Li, J., Diao, B., Guo, S., Huang, X., Yang, C., Feng, Z., … Wu, Y. (2017). VSIG4 inhibits proinflammatory macrophage activation by reprogramming mitochondrial pyruvate metabolism. *Nature Communications*, *8*, 1322. https://doi.org/10.1038/s41467-017-01327-4

Li, Y., Zhang, P., Wang, C., Han, C., Meng, J., Liu, X., … Cao, X. (2013). Immune responsive gene 1 (IRG1) promotes endotoxin tolerance by increasing A20 expression in macrophages through reactive oxygen species. *The Journal of Biological Chemistry*, *288*, 16225–16234. https://doi.org/10.1074/jbc.M113.454538

Livak, K. J., & Schmittgen, T. D. (2001). Analysis of relative gene expression data using real-time quantitative PCR and the $2^{-\Delta\Delta C}{}_T$ method. *Methods*, *25*, 402–408. https://doi.org/10.1006/meth.2001.1262

Miranda, A. S., Brant, F., Rocha, N. P., Cisalpino, D., Rodrigues, D. H., Souza, D. G., … Campos, A. C. (2013). Further evidence for an anti-inflammatory role of artesunate in experimental cerebral malaria. *Malaria Journal*, *12*, 388. https://doi.org/10.1186/1475-2875-12-388

Morizono, K., Xie, Y., Ringpis, G. E., Johnson, M., Nassanian, H., Lee, B., … Chen, I. S. Y. (2005). Lentiviral vector retargeting to P-glycoprotein on metastatic melanoma through intravenous injection. *Nature Medicine*, *11*, 346–352. https://doi.org/10.1038/nm1192

Orlov, I., Rochel, N., Moras, D., & Klaholz, B. P. (2012). Structure of the full human RXR/VDR nuclear receptor heterodimer complex with its DR3 target DNA. *The EMBO Journal*, *31*, 291–300. https://doi.org/10.1038/emboj.2011.445

Prucha, M., Zazula, R., & Russwurm, S. (2017). Immunotherapy of sepsis: Blind alley or call for personalized assessment? *Archivum Immunologiae et Therapiae Experimentalis (Warsz)*, *65*, 37–49. https://doi.org/10.1007/s00005-016-0415-9

Putzu, A., Belletti, A., Cassina, T., Clivio, S., Monti, G., Zangrillo, A., & Landoni, G. (2017). Vitamin D and outcomes in adult critically ill patients. A systematic review and meta-analysis of randomized trials. *Journal of Critical Care*, *38*, 109–114. https://doi.org/10.1016/j.jcrc.2016.10.029

Ren, C., Zhang, H., Wu, T. T., & Yao, Y. M. (2017). Autophagy: A potential therapeutic target for reversing sepsis-induced immunosuppression. *Frontiers in Immunology*, *8*, 1832. https://doi.org/10.3389/fimmu.2017.01832

Rittirsch, D., Huber-Lang, M. S., Flierl, M. A., & Ward, P. A. (2009). Immunodesign of experimental sepsis by cecal ligation and puncture. *Nature Protocols*, *4*, 31–36. https://doi.org/10.1038/nprot.2008.214

Ru, J., Li, P., Wang, J., Zhou, W., Li, B., Huang, C., … Yang, L. (2014). TCMSP: A database of systems pharmacology for drug discovery from herbal medicines. *Journal of Cheminformatics*, *6*, 13. https://doi.org/10.1186/1758-2946-6-13

Rudick, C. P., Cornell, D. L., & Agrawal, D. K. (2017). Single versus combined immunoregulatory approach using PD-1 and CTLA-4 modulators in controlling sepsis. *Expert Review of Clinical Immunology*, *13*, 907–919. https://doi.org/10.1080/1744666X.2017.1357469

Schaaf, M. B., Keulers, T. G., Vooijs, M. A., & Rouschop, K. M. (2016). LC3/GABARAP family proteins: Autophagy-(un)related functions. *The FASEB Journal*, *30*, 3961–3978. https://doi.org/10.1096/fj.201600698R

Singer, M., Deutschman, C. S., Seymour, C. W., Shankar-Hari, M., Annane, D., Bauer, M., … Angus, D. C. (2016). The third international consensus definitions for sepsis and septic shock (sepsis-3). *Jama-Journal of the American Medical Association*, *315*, 801–810. https://doi.org/10.1001/jama.2016.0287

Skrupky, L. P., Kerby, P. W., & Hotchkiss, R. S. (2011). Advances in the management of sepsis and the understanding of key immunologic defects. *Anesthesiology*, *115*, 1349–1362. https://doi.org/10.1097/ALN.0b013e31823422e8

Steinbeck, C., Han, Y., Kuhn, S., Horlacher, O., Luttmann, E., & Willighagen, E. (2003). The Chemistry Development Kit (CDK): An open-source Java library for Chemo- and Bioinformatics. *Journal of Chemical Information and Computer Sciences*, *43*, 493–500. https://doi.org/10.1021/ci025584y

Sun, J. (2016). VDR/vitamin D receptor regulates autophagic activity through ATG16L1. *Autophagy*, *12*, 1057–1058. https://doi.org/10.1080/15548627.2015.1072670

Sun, J., Kong, J., Duan, Y., Szeto, F. L., Liao, A., Madara, J. L., & Li, Y. C. (2006). Increased NF-κB activity in fibroblasts lacking the vitamin D receptor. *American Journal of Physiology. Endocrinology and Metabolism*, *291*, E315–E322. https://doi.org/10.1152/ajpendo.00590.2005

Wang, J., Zhang, J., Shi, Y., Xu, C., Zhang, C., Wong, Y. K., … Lin, Q. (2017). Mechanistic investigation of the specific anticancer property of artemisinin and its combination with aminolevulinic acid for enhanced anticolorectal cancer activity. *ACS Central Science*, *3*, 743–750. https://doi.org/10.1021/acscentsci.7b00156

Wu, S., Liao, A. P., Xia, Y., Li, Y. C., Li, J. D., Sartor, R. B., & Sun, J. (2010). Vitamin D receptor negatively regulates bacterial-stimulated NF-κB activity in intestine. *The American Journal of Pathology*, *177*, 686–697. https://doi.org/10.2353/ajpath.2010.090998

Wu, S., & Sun, J. (2011). Vitamin D, vitamin D receptor, and macroautophagy in inflammation and infection. *Discovery Medicine*, *11*, 325–335.

Wu, S., Zhang, Y. G., Lu, R., Xia, Y., Zhou, D., Petrof, E. O., … Sun, J. (2015). Intestinal epithelial vitamin D receptor deletion leads to defective autophagy in colitis. *Gut*, *64*, 1082–1094. https://doi.org/10.1136/gutjnl-2014-307436

Zheng, C., Guo, Z., Huang, C., Wu, Z., Li, Y., Chen, X., … Wang, Y. (2015). Large-scale direct targeting for drug repositioning and discovery. *Scientific Reports*, *5*, 11970. https://doi.org/10.1038/srep11970

SUPPORTING INFORMATION

Additional supporting information may be found online in the Supporting Information section at the end of this article.

How to cite this article: Shang S, Wu J, Li X, et al. Artesunate interacts with the vitamin D receptor to reverse sepsis-induced immunosuppression in a mouse model via enhancing autophagy. *Br J Pharmacol*. 2020;177:4147–4165. https://doi.org/10.1111/bph.15158